U. S. DEPARTMENT OF COMMERCE
ENVIRONMENTAL SCIENCE SERVICES ADMINISTRATION
WEATHER BUREAU

WEATHER BUREAU TECHNICAL MEMORANDUM SR-39

THE RELATIONSHIP OF PRECIPITATION AND CLOUDINESS TO SOME PREDICTORS FROM THE NMC SIX-LAYER MODEL

SOUTHERN REGION HEADQUARTERS
SCIENTIFIC SERVICES DIVISION
TECHNICAL MEMORANDUM NO. 39

FORT WORTH, TEXAS
October 1968

TABLE OF CONTENTS

THE RELATIONSHIP OF PRECIPITATION AND CLOUDINESS TO SOME PREDICTORS FROM THE NMC SIX-LAYER MODEL

Staff, Scientific Services Division

INTRODUCTION

Implementation of the six-layer primitive equation model at the National Meteorological Center (NMC) in mid-1966 opened the way for the production, on a physically-sound basis, of a number of predictors expected to be useful in forecasting cloudiness and precipitation.(1,2) These are used, objectively and subjectively, to produce NMC forecasts which appear on facsimile in various formats, including the depiction of predicted weather at specified synoptic times and forecast precipitation probabilities and amounts for certain periods. (3,4)

The availability of a large number of quality prognostic charts and forecasts has not, however, obviated the necessity for the field forecaster to add detail, in time and space, to the guidance forecasts. Aside from short-term extrapolation and consideration of local effects, such as orography, it seems likely that the best opportunity for supplementing guidance received from NMC is through judicious use of some of the numerically derived parameters which are routinely available. For this, the forecaster needs objective techniques and an understanding of the behavior and effects of the predictors. Such a calibration on a regional basis - the content of this memorandum - is intended to provide some assistance toward using the products more systematically. Emphasis will be principally on Mean Relative Humidity ($\overline{RH}$), Vertical Velocity (VV), and Lifted Index (LI). A short discussion on utilization of information from the Techniques Development Laboratory Sub-synoptic Advective Model (5) is included as an Annex.

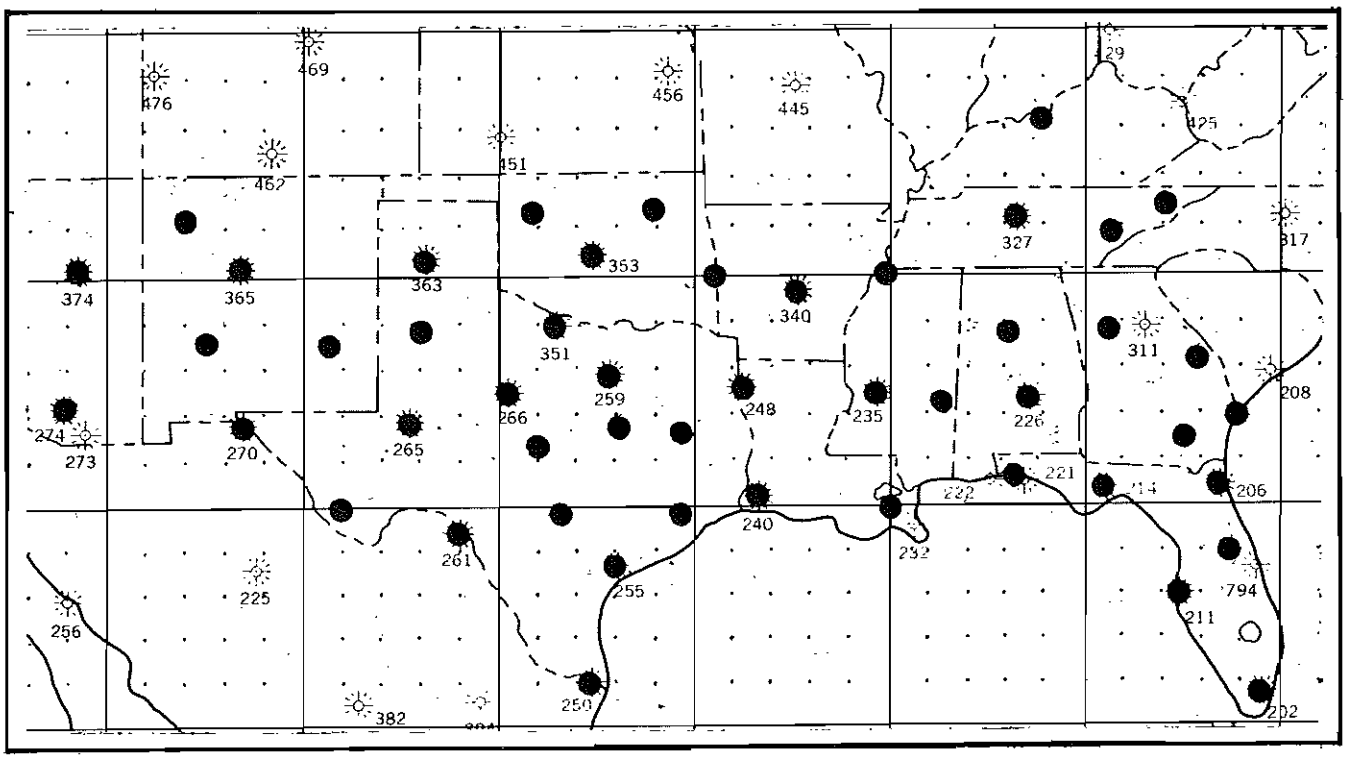

P E PARAMETER NETWORK

Figure 1

DATA USED IN STUDY

In evaluating the utility of $\overline{RH}$, VV, and LI, data from a network of 50 stations in the Weather Bureau Southern Region (Figure 1) were examined. The periods covered were May, June, November, and December of 1967 and March, April, and May of 1968. Values of $\overline{RH}$, VV, and LI were interpolated from facsimile charts for the initial and 24-hour forecasts of these parameters. Precipitation data were recorded as zero, trace, or measurable amount for the 6-hour period ending at 00Z and 12Z.

During the period covered by the data collection, several changes were made in the primitive equation model. The earlier $\overline{RH}$ values used in the study were adjusted to take into consideration some changes in saturation criteria and a normalization of $\overline{RH}$ values in the output format. It was not feasible to make allowance for model changes which have affected vertical motion fields, particularly initial values.

The sampling periods and model changes are shown in Figure 2.

DATA USED IN STUDY AND SIGNIFICANT CHANGES IN THE NWP PE MODEL

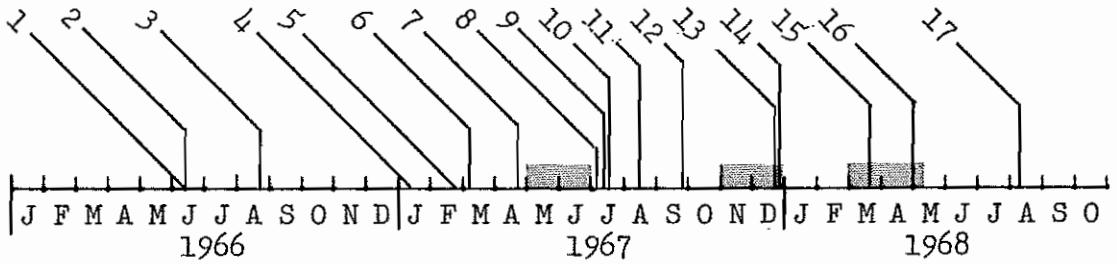

Blocks represent data periods used in study
Numbers indicate model changes listed below

1. 12Z June 6, 1966 - First run of model (6)
2. 12Z June 13, 1966 - Inconsistency in finite differences corrected (6)
3. 12Z Aug. 16, 1966 - Boundary layer cooling over snow fields introd.(6)
4. 12Z Jan. 2, 1967 - Precipitation forecasts introduced (6)
5. 12Z Feb. 20, 1967 - Latent heat fed into temperature forecasts (6)
6. 12Z March 7, 1967 - Two-sigma-layer moist convective adjustments fed into temperature forecasts (6)
7. 12Z April 20, 1967 - Observed sea-surface temp. analysis introduced (6)
8. 12Z July 5, 1967 - Heating and cooling, boundary layer thickness changed (7)
9. 12Z July 12, 1967 - Seasonal (May-Sept) saturation criteria introduced (8)
10. 12Z July 17, 1967 - Mean RH charts on Fax normalized for Seasons (9)
11. 12Z Aug. 23, 1967 - Precip. included in moisture analysis (10)
12. 12Z Sept. 26,1967 - Sea level pressure forecasts, computed by tendency method (11)
13. 12Z Dec. 22, 1967 - Lapse rate adjustments incorporated (12)
14. 00Z Dec. 29, 1967 - 12-hr. forecast mean $\overline{RH}$ used as first guess at grid points (10)
15. 12Z Mar. 13, 1968 - Improvement in vertical moisture distribution effected (13)
16. 12Z April 29, 1968 - Divergent initialization of PE model (14)
17. 12Z Aug. 6, 1968 - Surface topography in model changed (15)

Figure 2

SEASONAL AND GEOGRAPHICAL FACTORS

Although the data did not include an entire year, a good indication of the seasonal variability of $\overline{RH}$, VV, and LI was obtained, as shown in Figure 3. The $\overline{RH}$ distributions for the November-December data indicate a greater frequency of extremes i.e., $\leq 40\%$ and $>90\%$, than May-June information and the latter shows a peak in the 70-80% grouping (Figure 3a). LI values (Figure 3b) tend toward stability in the winter and instability in May-June much as would be expected. A slightly greater frequency of VV values $\geq +1$ microbars per second is shown for winter than early summer Figure 3c).

It was initially expected that there would be geographical variations in the relationships between the predictors and the frequency of precipitation. In order to test this, the data were separated into samples for the areas east and west of a line extending from Tulsa, Oklahoma to Brownsville, Texas, delineating areas of different climatic regimes and precipitation frequencies. There was considerable difference in the frequency distribution of the parameters in the two samples but no obvious areal variation in the correlation of the values of the parameters with precipitation. The data were therefore combined in order to gain a larger sample size. It is believed that the results of the study are not highly areally-dependent.

DISTRIBUTION AND ANALYSIS OF THE PARAMETERS

Bar graphs were prepared showing the frequency of occurrence of $\overline{RH}$, LI, and VV by stratifications of the initial and 24-hour forecast parameters. Others demonstrate the specifying capability of these stratifications for frequency of precipitation amounts equal to or greater than .01 inch. The distribution of initial and forecast fields of $\overline{RH}$ is shown in Figure 4a. Initial $\overline{RH}$ values were most frequent around 60%. This peak in the distribution was flattened considerably by the prediction mechanics of the PE model as can be seen by the comparison of the bars within $\overline{RH}$ classes in Figure 4a.

The comparison of initial and forecast $\overline{RH}$ categories for specifying precipitation (.01 inch or greater) is shown in Figure 4b. The graph shows good discrimination of $\overline{RH}$ fields for specifying precipitation. Thus a 44% probability was found with initial values of $\overline{RH}$ equal to or greater than 90% which deteriorated to 34% with the same forecast $\overline{RH}$ values. Precipitation frequency dropped to 12% and 13% respectively for initial and forecast $\overline{RH}$ values of 70% to 80% and to less than 5% for all categories of $\overline{RH}$ equal to or less than 60%.

A study of Figure 4b shows the effects of errors in $\overline{RH}$ forecasts on probability of precipitation forecasting. The month by month, or seasonal, variation in the distribution of $\overline{RH}$ and its correlation with frequency of precipitation was not significant, justifying the inclusion of the entire sample of data (over 15,600 occurrences) into Figures 4a and 4b.

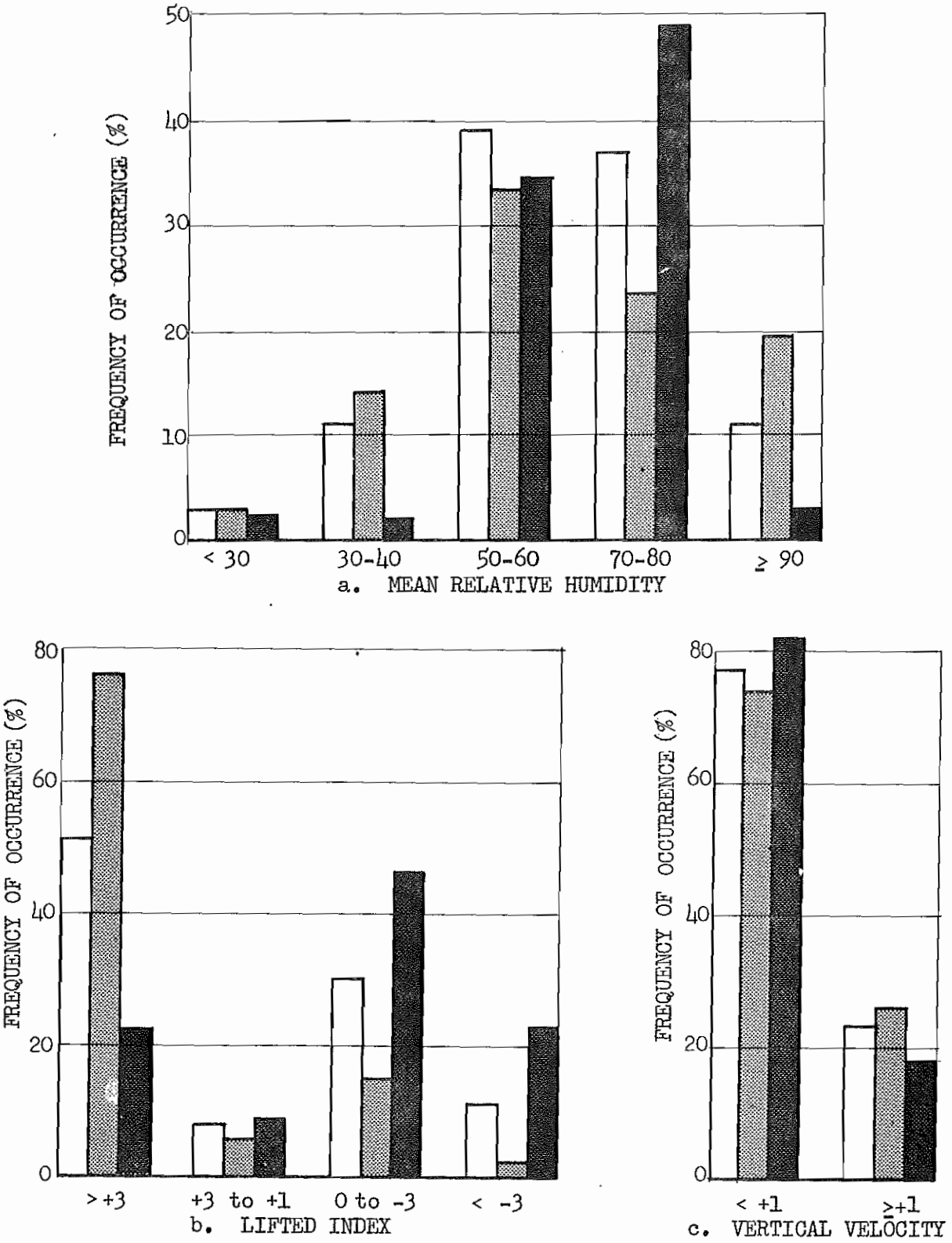
FREQUENCY OF OCCURRENCE (%)
50
40
30
20
10
0
< 30
30-40
50-60
70-80
≥ 90
a. MEAN RELATIVE HUMIDITY
FREQUENCY OF OCCURRENCE (%)
80
60
40
20
0
> +3
+3 to +1
0 to -3
< -3
b. LIFTED INDEX
FREQUENCY OF OCCURRENCE (%)
80
60
40
20
0
< +1
≥+1
c. VERTICAL VELOCITY
7 Months' Data
NOV.- DEC. '67
MAY-JUNE '67

Figure 3

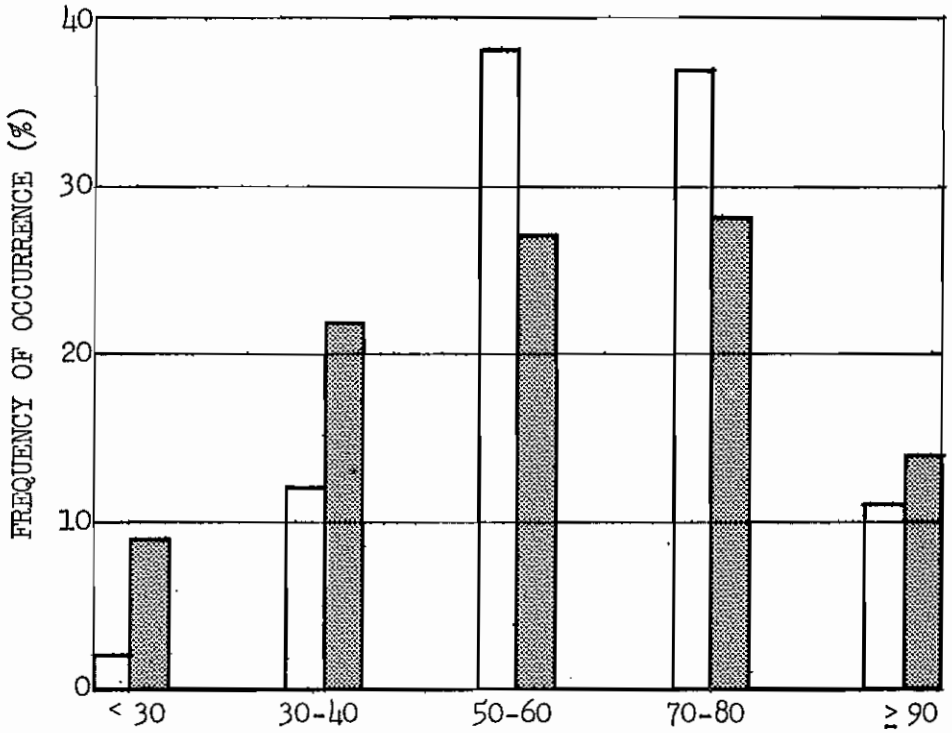

a. MEAN RELATIVE HUMIDITY

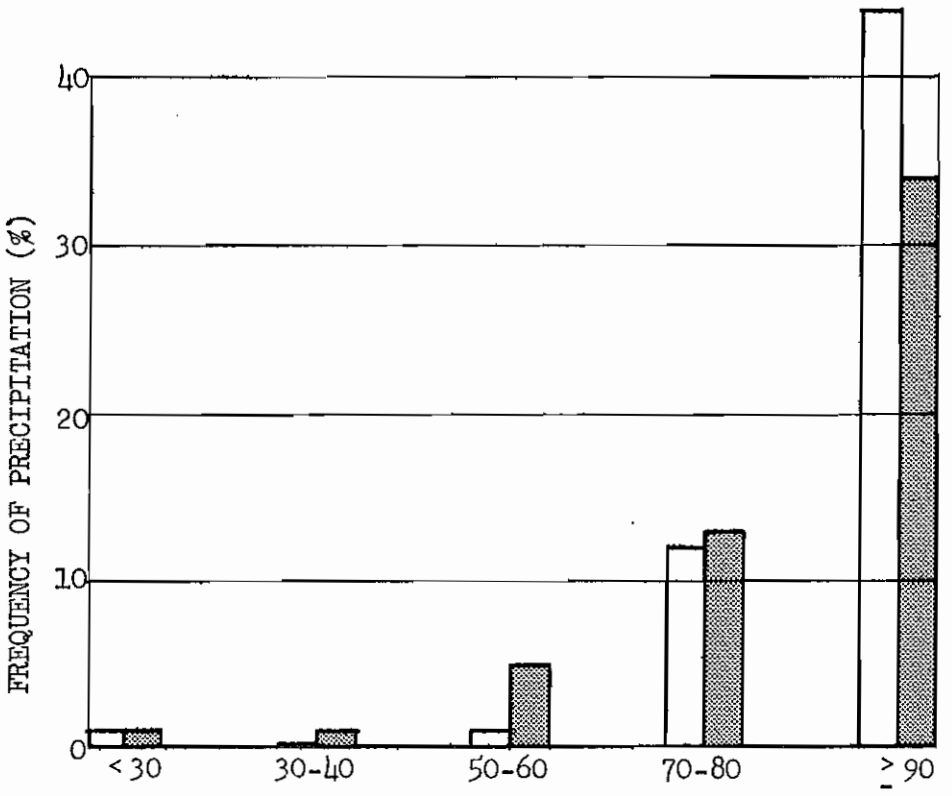

b. MEAN RELATIVE HUMIDITY

INITIAL FORECAST

Figure 4

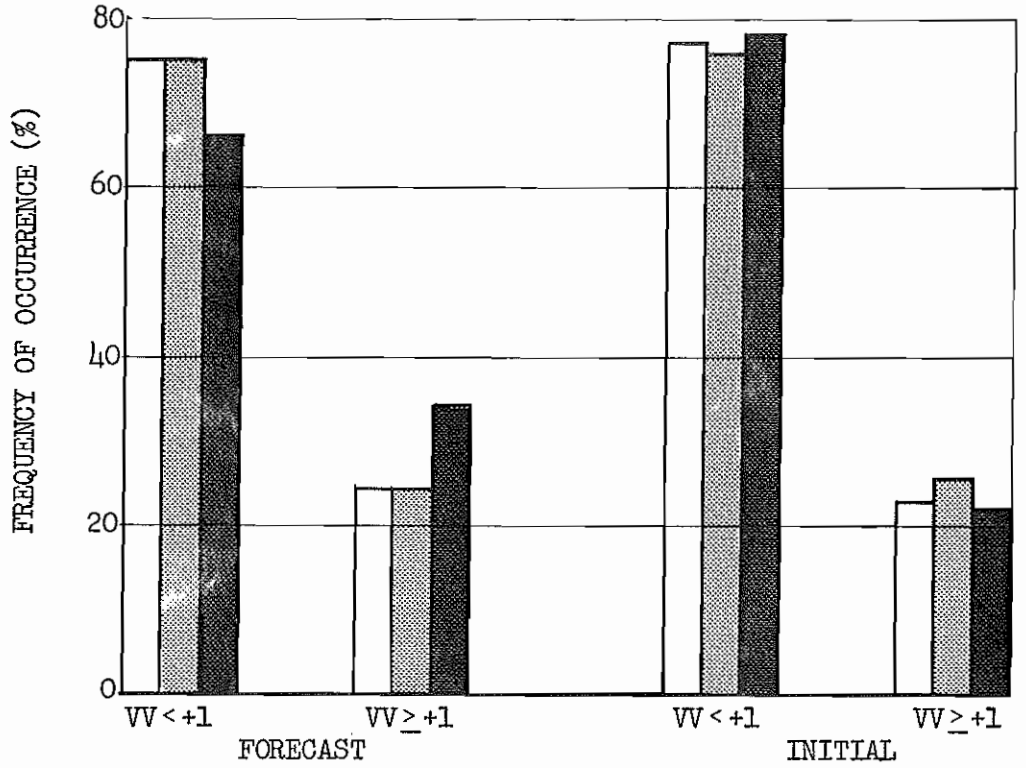

a.

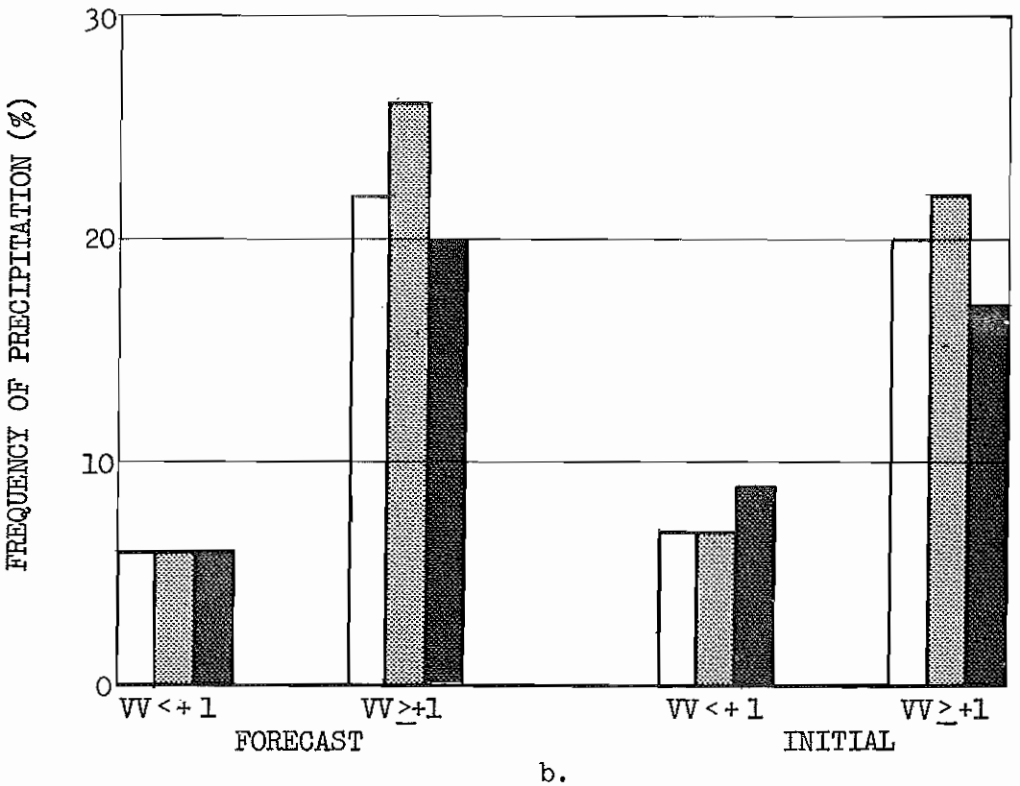

b.

7 Months' Data NOV.-DEC.'67 APR.-MAY '68

Figure 5

The distribution of VV values less than one microbar per second and equal to or greater than one is shown in Figure 5a and the relationship of these categories of VV to frequency of precipitation ($\geq$ .01") in Figure 5b. Seasonal effects are available from a comparison of the November-December '67 bars with those for April-May '68. Appropriate distributions of VV are labeled "Initial" although these actually are 6-hour forecasts corresponding to the first panel on facsimile depiction charts. Data arrays not shown indicated that zero VV values occurred about half the time. The selection of +1 VV in this part of the study as a boundary between classes to represent "upward" and "downward" atmospheric motion was made subjectively after surveying various data samples for precipitation discriminating features. It can be seen in Figure 5a that three-fourths of the data fall in the "downward" motion category for initial and forecast conditions. On the other hand, the frequency of precipitation is near 20% for VV $\geq$ +1. The forecast values of VV indicate precipitation probability slightly better than initial conditions and appear to be more discriminatory in winter than in the warmer season.

The classes of LI displayed in Figures 6 and 7 were selected after experimentation for precipitation specifying capability of several regimes. The occurrence distribution (Figure 6a) is bi-modal showing one peak for stable conditions (>+3) and another for slightly unstable conditions (0 to -3 inclusive). Values of LI less than -3 are relatively rare in the sample as a whole and even for the April-May data. The large +3 class contains values ranging to above +20 and is dominant in the winter season.

The bi-modal feature in the occurrence of classes appears in the forecast values (Figure 6b), and the frequency of 24-hour forecast values by classes compares well with the observed for each seasonal sample displayed in Figure 6a.

For the initial LI data in Figure 7a, a greater propensity for precipitation is indicated as conditions range from stable to unstable. In the comparable forecast data of Figure 7b the discrimination is degraded in the winter data but amplified in the April-May '68 information.

COMPARISON OF PREDICTORS

Mean Relative Humidity computations and forecasts were indicated to be the strongest predictors of precipitation among the PE parameters considered. Analyses gave 44% frequency of measurable precipitation when $\overline{RH}$ was equal to or greater than 90%. This condition existed only 11% of the time. Rain frequency at 70 to 80% humidity was only 12%, and, for $\overline{RH}$ less than 70%, rain frequency was only about 1%. Forecasts of $\overline{RH}$ and the frequency of precipitation associated with $\overline{RH} \geq 90$ held up well with 34% probability of precipitation indicated for this class.

24-hour forecasts of VV $\geq$ +1 microbars per second gave 22% precipitation frequency vs 6% for VV<+1. A similar trend was indicated for LI with precipitation frequency rising from 6% for the most stable classification to 18% for the most unstable category.

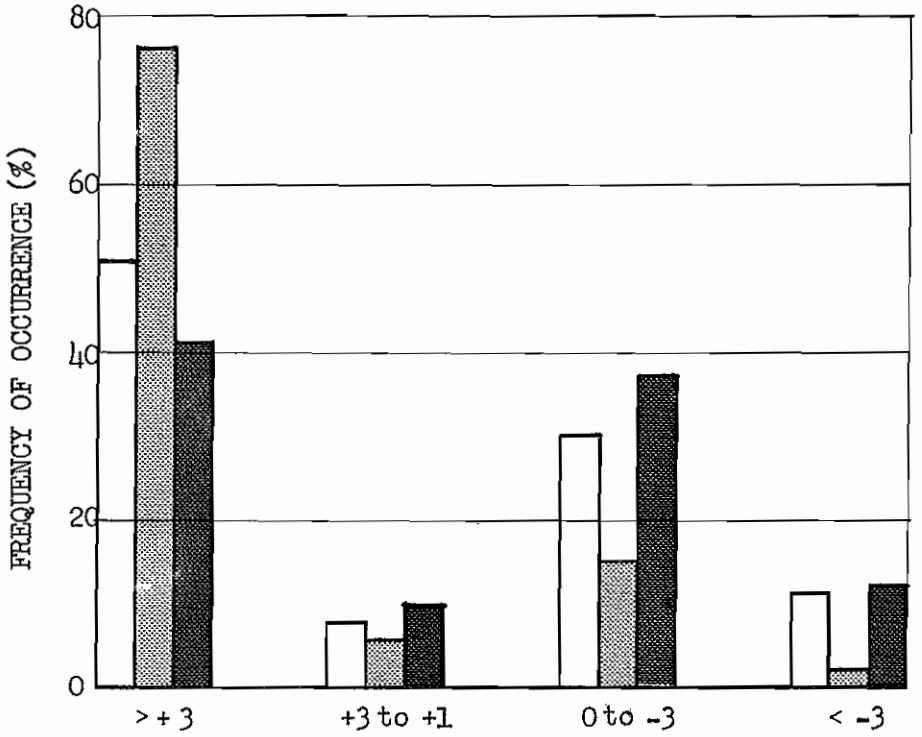

a. INITIAL LIFTED INDEX

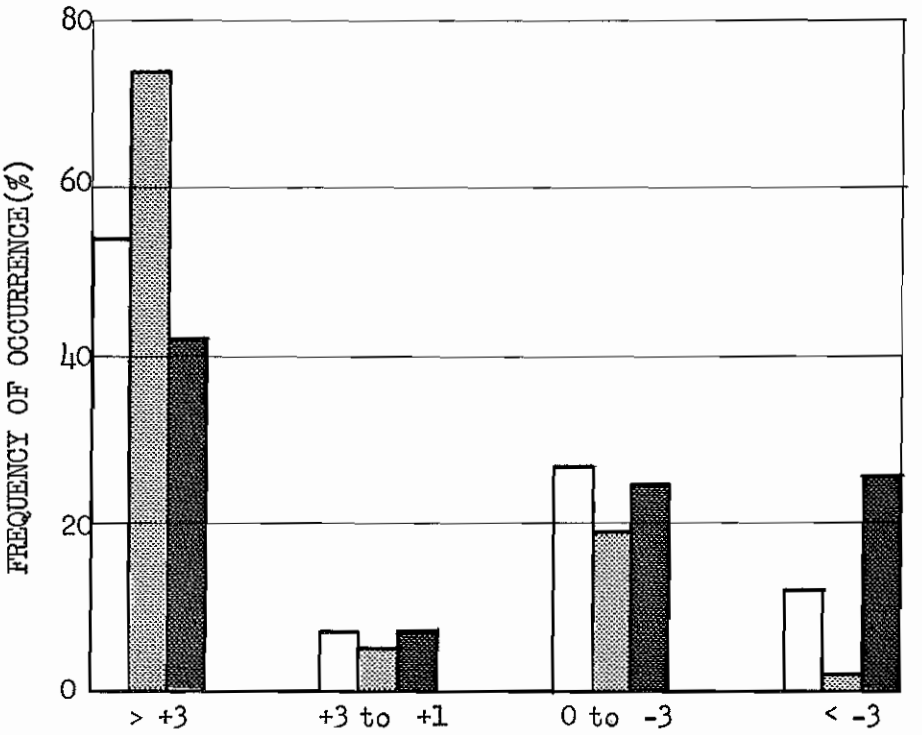

b. 24 HOUR FORECAST
LIFTED INDEX

7 Months' Data NOV.-DEC. '67 APRIL-MAY '68

Figure 6

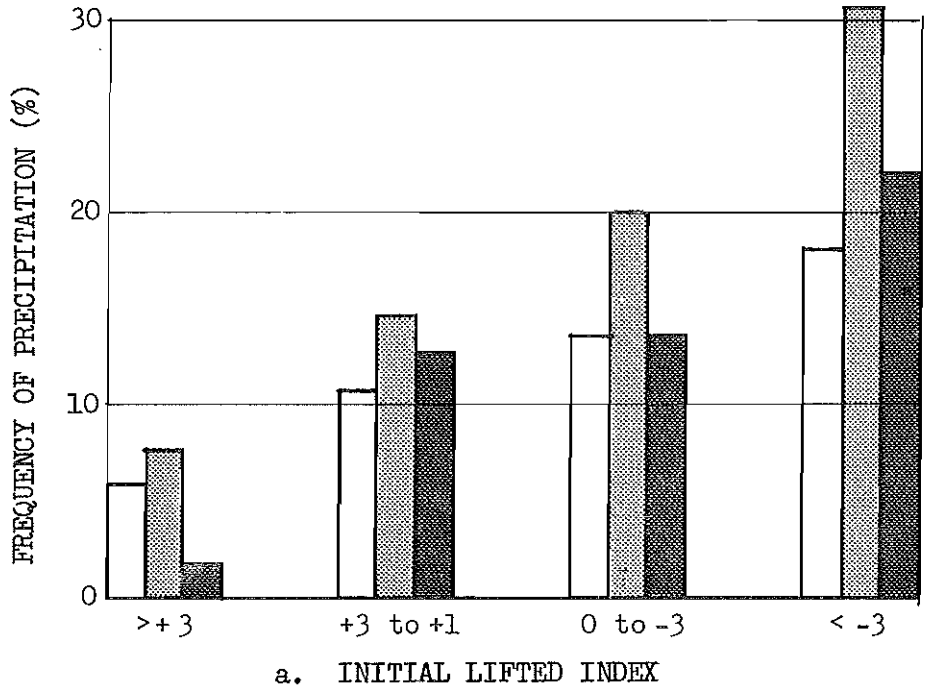

a. INITIAL LIFTED INDEX

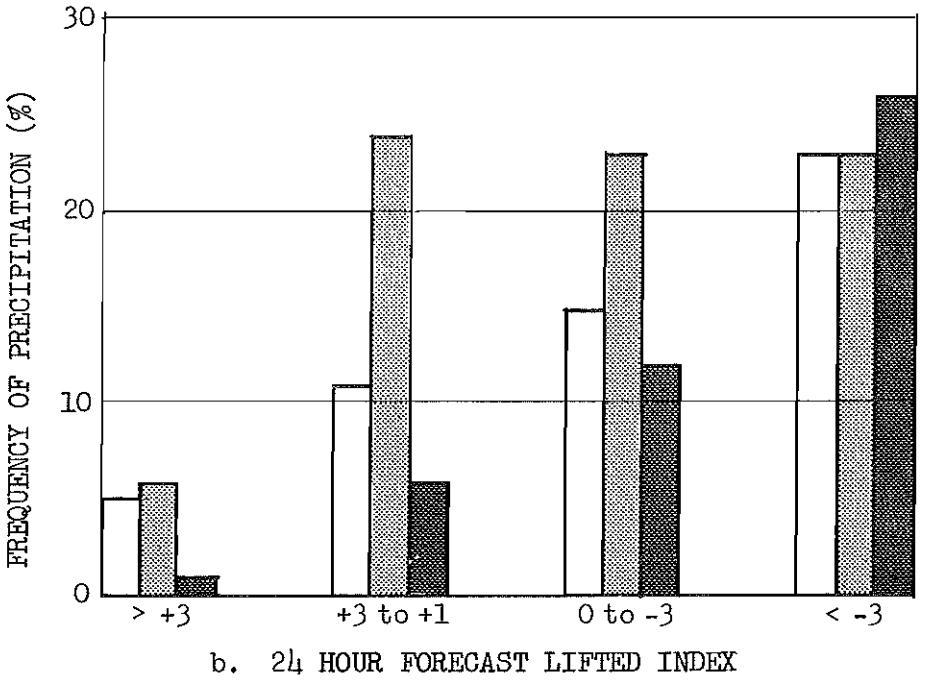

b. 24 HOUR FORECAST LIFTED INDEX

7 Months' Data NOV.-DEC. '67 APRIL-MAY '68

Figure 7

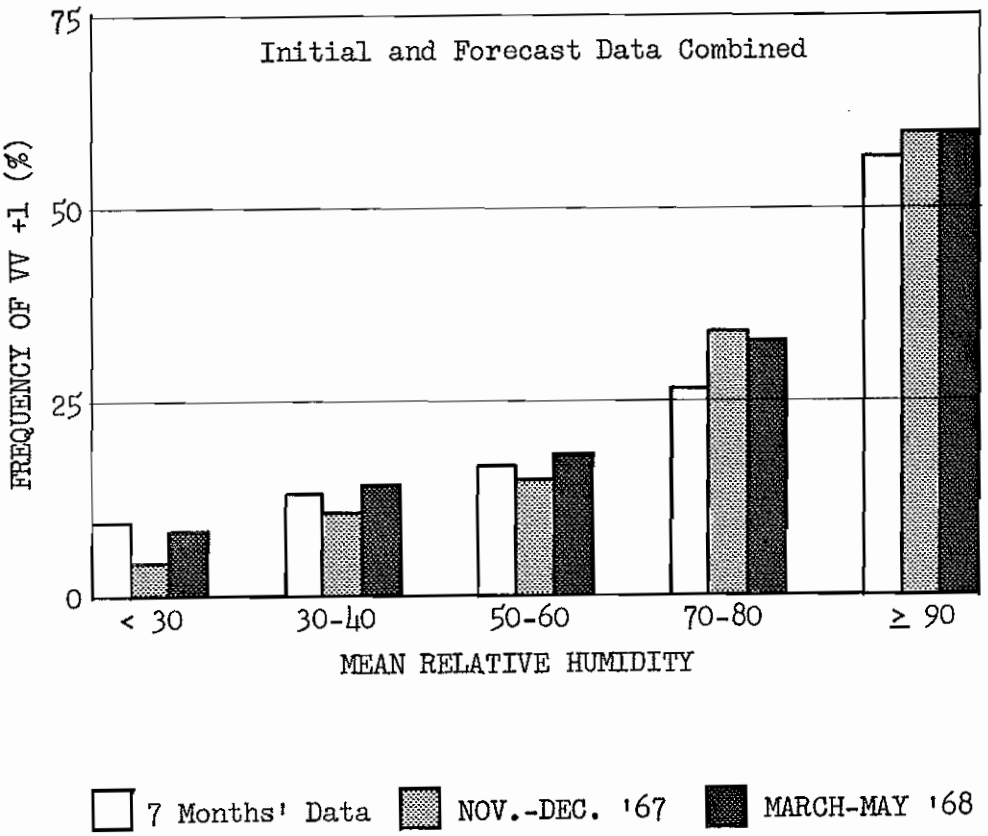

Figure 8

INTERDEPENDENCE OF PARAMETERS

The degree of mutual independence of RH, VV, and LI should determine the advantage of considering in concert the various predictors for forecasting occurrences of precipitation.

Figure 8 illustrates the association between $\overline{RH}$ and VV for combined initial and forecast conditions. The frequency of $\overline{VV}$ values $\geq +1$ increases as $\overline{RH}$ increases. This should be expected since VV represents instantaneous vertical motion while sustained vertical motion favors higher $\overline{RH}$ values in both initial and forecast fields.

Figure 9 shows the correspondence between $\overline{RH}$ and classes of Lifted Index, again for combined initial and 24-hour forecast data. Stable conditions predominate with low humidity but the tendency is for instability to be more frequent with moist conditions. This tendency is much more pronounced March through May than in the November-December period. Thus one concludes that VV and LI values are correlated with Mean Relative Humidity and that forecast information contained in one of the parameters may be redundant in the other.

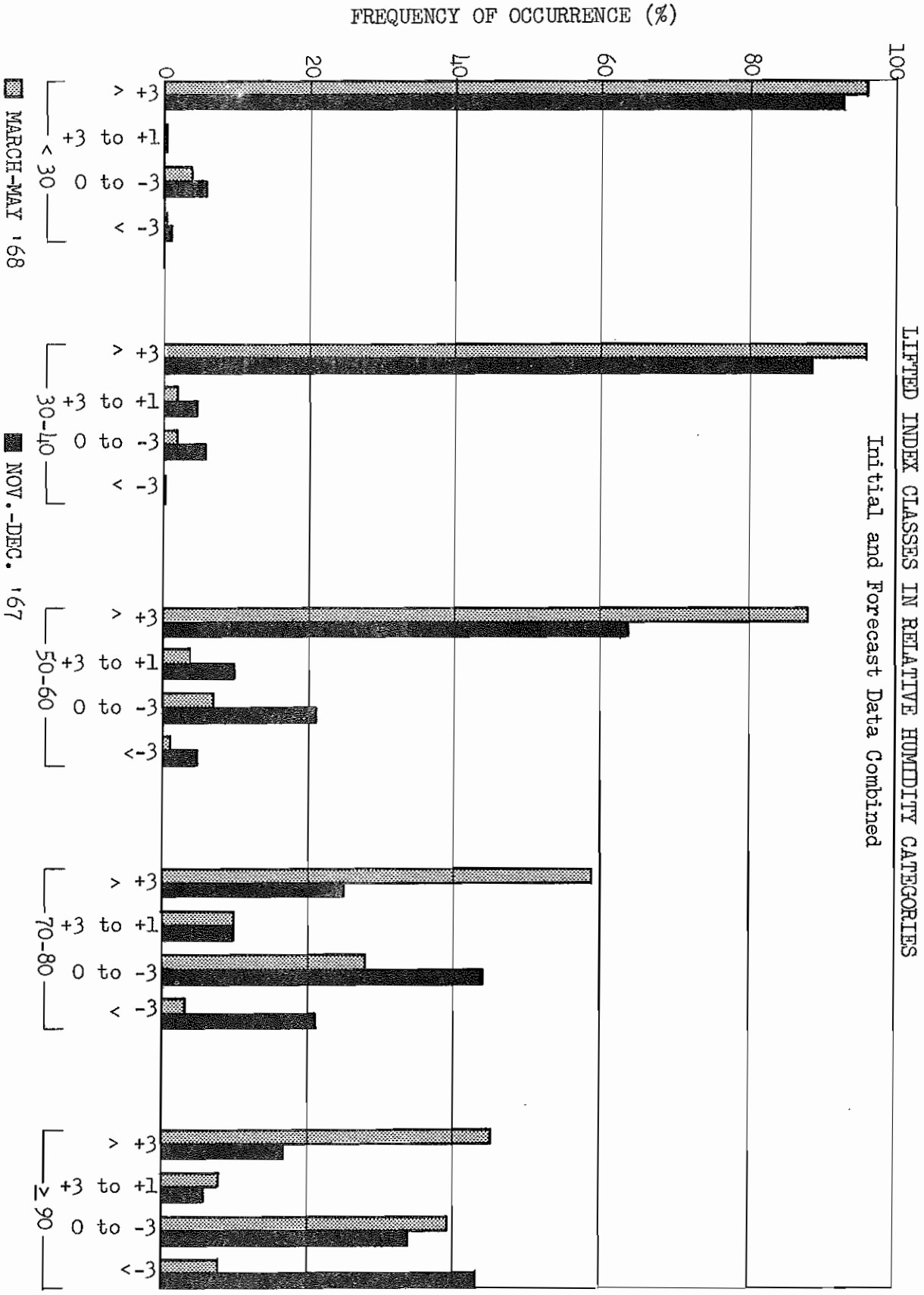
FREQUENCY OF OCCURRENCE (%)
0
20
40
60
80
100
LIFTED INDEX CLASSES IN RELATIVE HUMIDITY CATEGORIES
Initial and Forecast Data Combined
MARCH-MAY '68
NOV.-DEC. '67
< 30
30-40
50-60
70-80
≥ 90
> +3
+3 to +1
0 to -3
< -3
<-3

Figure 9

Figure 10 compares frequency of VV ≥+1 and Lifted Index. The general trend is for "upward" motion to become dominant as instability increases. While the overall frequency for VV ≥+1 is only about 25% in November-December, Figure 5a, this frequency goes above 60% when LI is less than -3. Such unstable conditions, however, are relatively rare in winter (Figure 6). Thus VV and LI not only are dependent on $\overline{RH}$ but are mutually related to a significant degree.

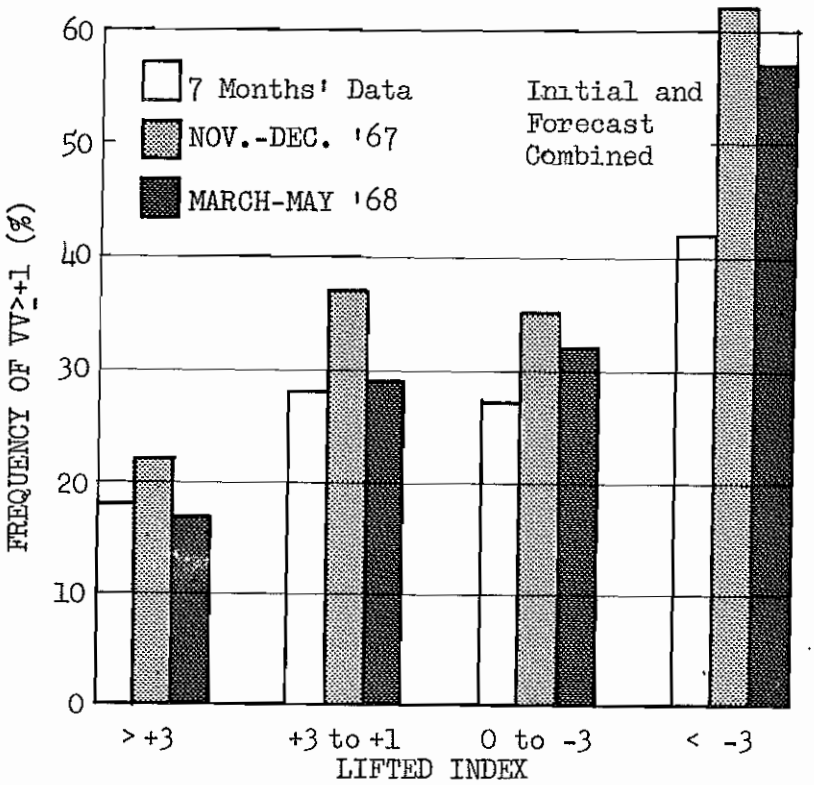

Figure 10

COMBINING PARAMETERS

Three-way Combination of predictors to jointly assess the effects of $\overline{RH}$, VV, and LI on the likelihood of precipitation would be very useful to forecasters, but the three have been shown to be related. Attempts were made to isolate the effect of a third parameter after considering two, but the variation of the residual from a two-way relation with the third parameter was found to vary in an apparent random manner, and yielded no significantly useful forecasting technique.

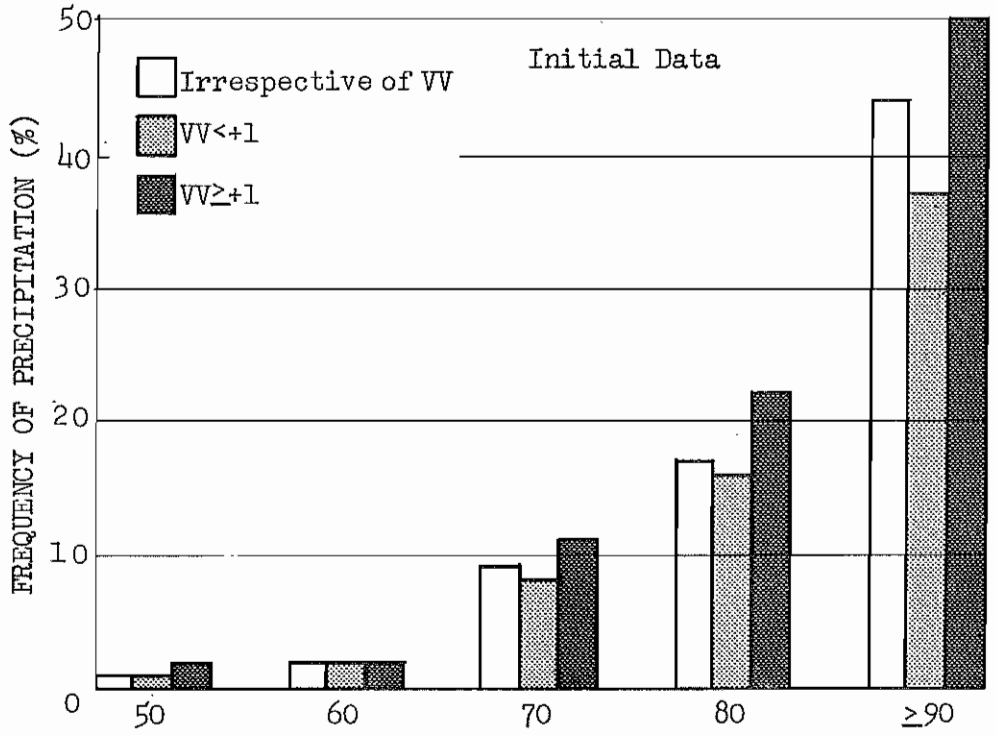

Figure 11

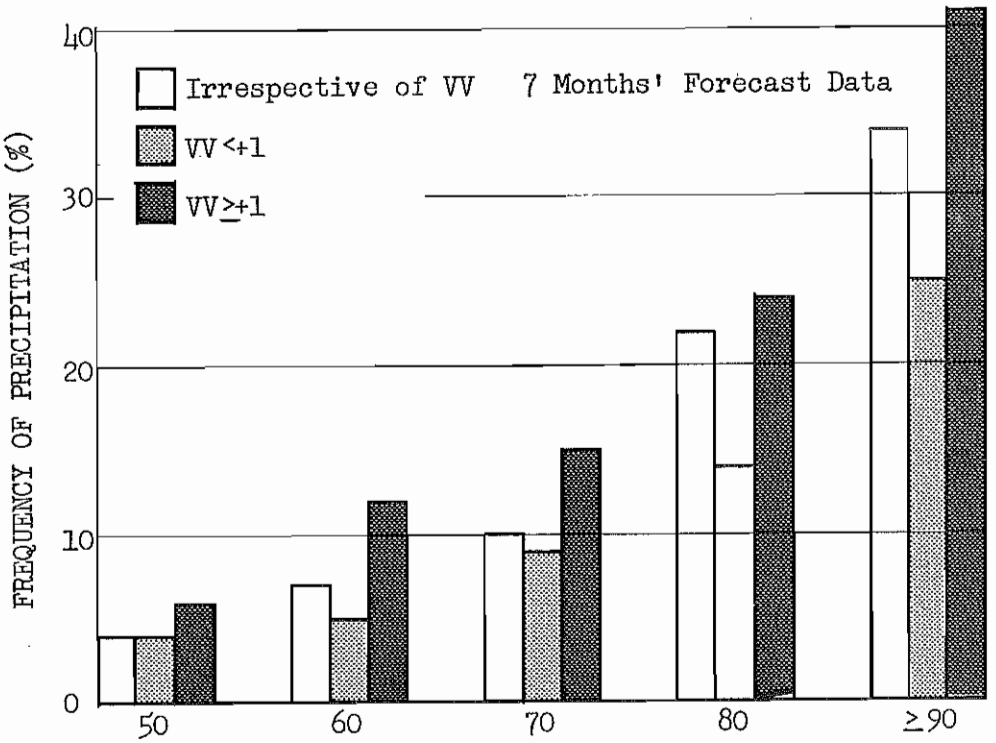

Figure 12

Two-way Combinations did indicate advantage to forecasters. The usefulness of VV in conjunction with $\overline{RH}$ to specify precipitation is indicated by Figures 11 and 12 using all available data. The 44% frequency of precipitation when $\overline{RH}$ is ≥ 90 increases to 50% if VV is $\geq +1$, and drops to 37% if VV is $< +1$ as shown by Figure 11 (initial data). The advantage of using VV decreases as $\overline{RH}$ becomes lower - 22% vs 16% chance of precipitation at 80% $\overline{RH}$, 11% vs 8% at 70% $\overline{RH}$, etc.. For forecast values (Figure 12) of $\overline{RH} \geq 90$, $VV \geq +1$ gives 41% chance of rain against 25% for $VV < +1$ and the advantage extends into lower $\overline{RH}$ categories. Thus one concludes there is definite advantage in precipitation forecasting in considering vertical velocity forecasts along with $\overline{RH}$ forecasts.

The winter data (Table 1) provides detail by $\overline{RH}$ classes on the association of large forecast values of VV with frequency of precipitation (%P). A striking result is 55% frequency within the class $VV \geq +2$. The frequency is 67% with $\overline{RH} \geq 90$. Good discrimination is shown as $\overline{RH}$ decreases. At the other extreme of $VV \leq -2$ precipitation occurred only once out of 297 cases.

TABLE 1
Nov.-Dec. '67 Forecast Data

	Mean Relative Humidity											
	<30		30-40		50-60		70-80		≥90		Σ	
VV	N	%P	N	%P	N	%P	N	%P	N	%P	N	%P
≥+2	5	0	10	10	19	32	50	36	179	67	263	55
+1	15	7	147	3	177	9	270	18	297	28	907	17
0,-1	524	1	1087	1	914	5	593	15	287	26	3405	6
≤-2	38	0	160	0	69	0	29	3	1	0	297	0
Σ	582	1	1404	1	1179	5	942	12	764	37	4871	11

To represent the cooler season, October through April, a graphical aid to forecasting using Mean Relative Humidity and Vertical Velocity was developed using a refinement of VV values to one microbar per second intervals. This graph is presented as Figure 26 in the section that follows on Use of Predictors in Forecasting Routine.

No satisfactory correlation was found between LI and winter precipitation. This was not altogether unexpected, for Lifted Index historically has been associated in forecasting practice with severe local storm forecasting - primarily a warm season (or at least a warm weather) phenomena.

Figure 13 displays the frequency of precipitation given by classes of Lifted Index within categories of $\overline{RH}$ for all initial data. More stable conditions are shown by the left bar within each humidity category.

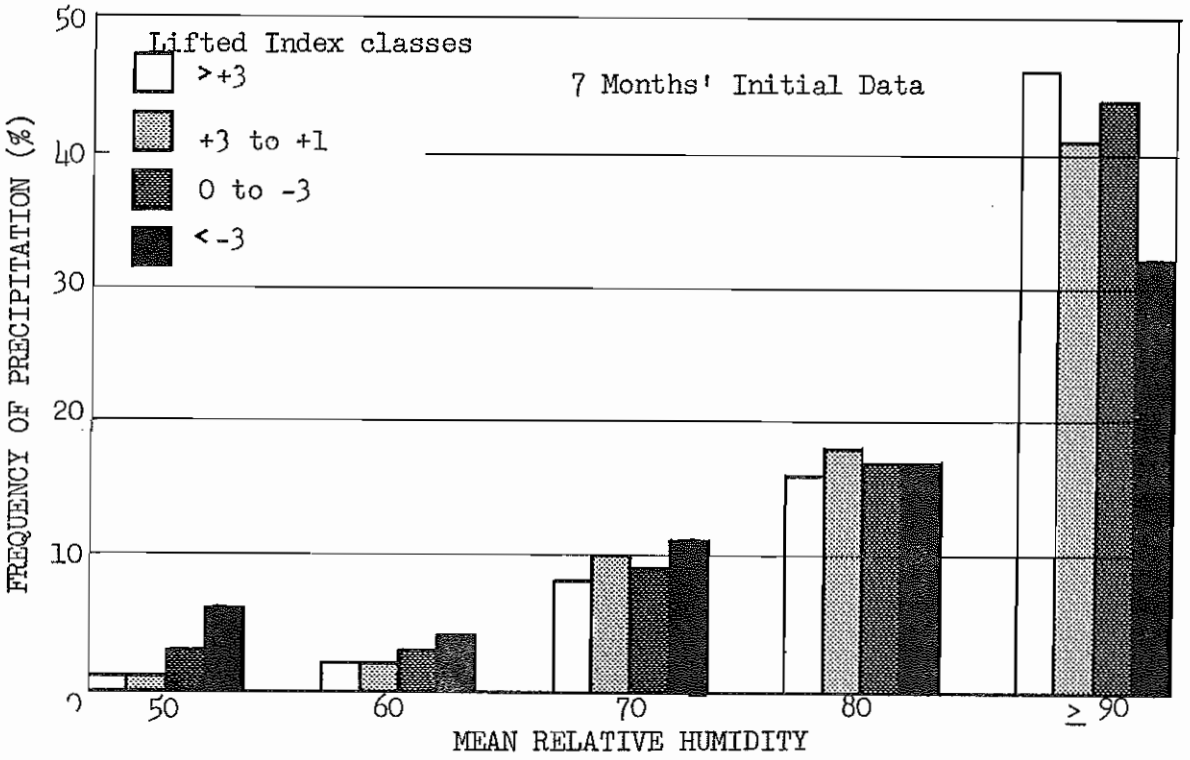

Figure 13

In the 50% $\overline{RH}$ category, precipitation frequency increases with increasing instability, and a similar trend can be noted for 60% and 70% $\overline{RH}$. At 80% $\overline{RH}$ precipitation freququency appears to be independent of the stability index, and for 90% or greater $\overline{RH}$, increasing instability appears to inhibit precipitation. This was an unexpected correlation, and was investigated further. The feature was found to be independent of the selected VV categories $<+1$ or $\geq +1$ microbars per second, and of seasonal samples as shown by Table 2.

TABLE 2
Frequency of Measurable Precipitation by Lifted Index Classes (with Mean Relative Humidity 90%)

	LI >+3	+3 to +1	0 to -3	≥ -3
May-June 1967	20	37	38	25
Nov.-Dec.1967	44	44	39	37
Mar.-Apr.1968	43	41	38	37

One suggested explanation of this apparent anomaly is that the 90% $\overline{RH}$ class includes many cases of general rains and relatively high probabilities but that the effect of increasing instability is a more showery character of precipitation and a lower point probability of rain.

Harned (16) studied interpolated lifted index values and thunderstorm occurrences at Tri City Airport, Tennessee for March-August 1965-68. His data shows a sharp drop in thundershower frequency with stability indices below zero, supporting the indications of this study that strong instability can result in lowered point rainfall probability.

DIURNAL VARIATIONS IN WARM SEASON

For warmer season forecasting use, stratification into 00Z and 12Z groups was useful in refinement of LI and VV contributions on a diurnal basis. Vertical motion was found to show a very poor correlation with afternoon shower activity during this season but both initial and forecast VV values for 12Z were well correlated with precipitation occurrence as shown in Figure 14.

Vertical motion appears to be able to explain as much as 15 to 20% difference in precipitation frequency for the higher relative humidity ranges. As Figure 15 shows, an extreme variation in lifted index can apparently account for a similar percentage of difference in frequency of precipitation for the afternoon period. The relationship of lifted index, forecast and observed, to early morning precipitation was rather erratic. The best combination of predictors for the warmer season therefore are $\overline{RH}$ and VV for the 12Z forecast time and $\overline{RH}$ in conjunction with LI for 00Z. The graphical forecasting aids corresponding to this conclusion appear as Figures 24 and 25 in Use of Predictors in Forecasting Routines.

FREQUENCY OF TRACE VS .01 INCH OF PRECIPITATION

The precipitation frequency for the entire period studied (expressed as .01 inch or more in the six-hours preceding synoptic time at which the predictors were valid) was 10%. Although the Weather Bureau precipitation forecast verification program is geared to .01 inch occurrences, trace amounts are also of interest and it was considered worthwhile to examine the relationship of the PE output variables to both measurable and trace amounts.

TABLE 3
Comparison of ≥Trace and ≥.01 in. Frequencies

		Mean Relative Humidity					
		≤40	50-60	70-80	≥90	All	
May-June '67	T	1%	4%	12%	44%	12%	
	.01	1%	3%	12%	36%	9%	
		≤40	50-60	≥70			
Nov.-Dec. '67	T	0	2%	36%		18%	
	.01	0	1%	23%		11%	
		Lifted Index				Vertical Velocity	
		>+3	+3 to 1	0 to -3	<-3	<+1	≥+1
May-June '67	T	3%	7%	13%	21%	11%	15%
	.01	2%	5%	10%	15%	8%	13%
Nov.-Dec. '67	T	13%	27%	30%	48%	11%	37%
	.01	8%	15%	20%	32%	7%	24%

The comparative frequency of trace and .01 inch showed a slight seasonal variation with 12% versus 9% in May and June and 18% versus 11% in November and December.

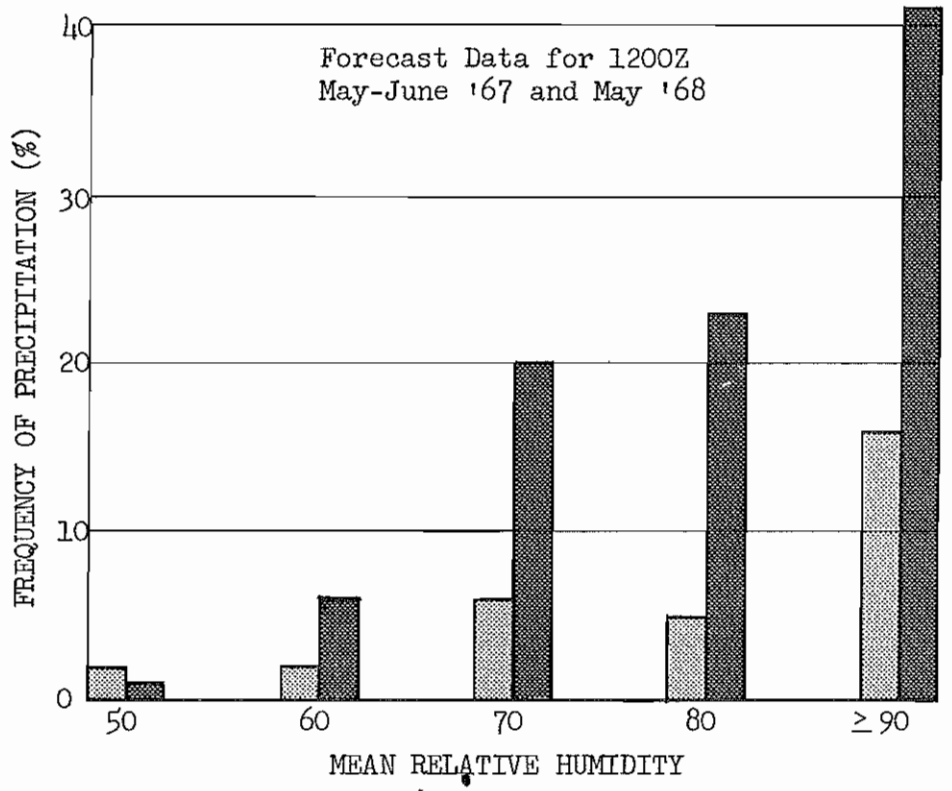

a.

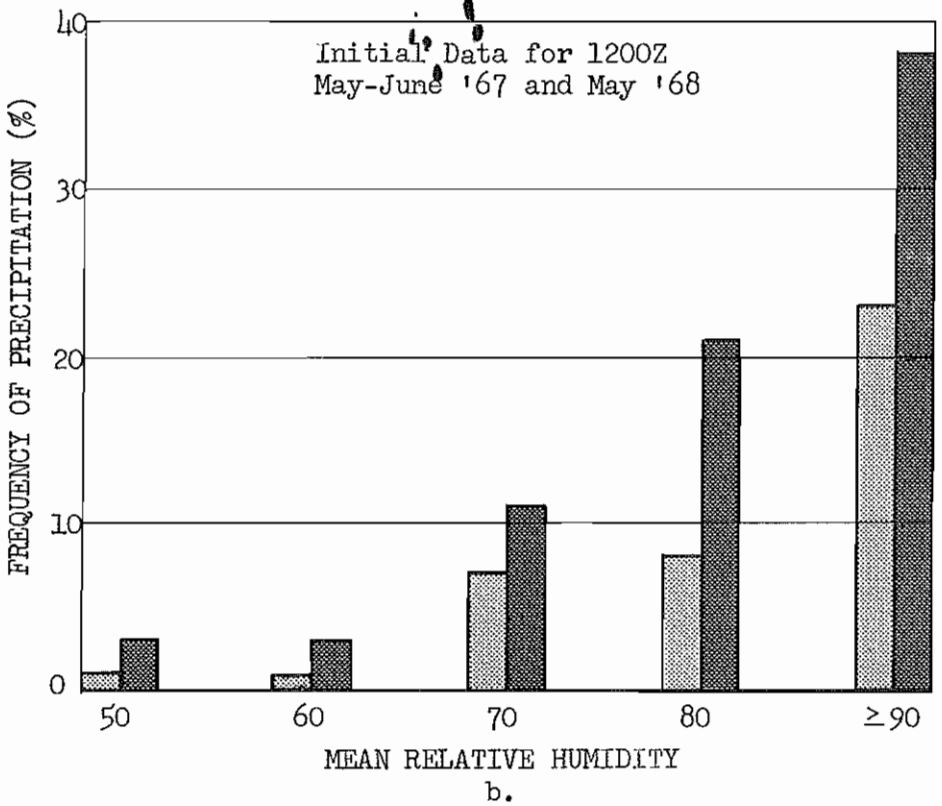

b.

VV < +1 VV ≥ +1

Figure 14

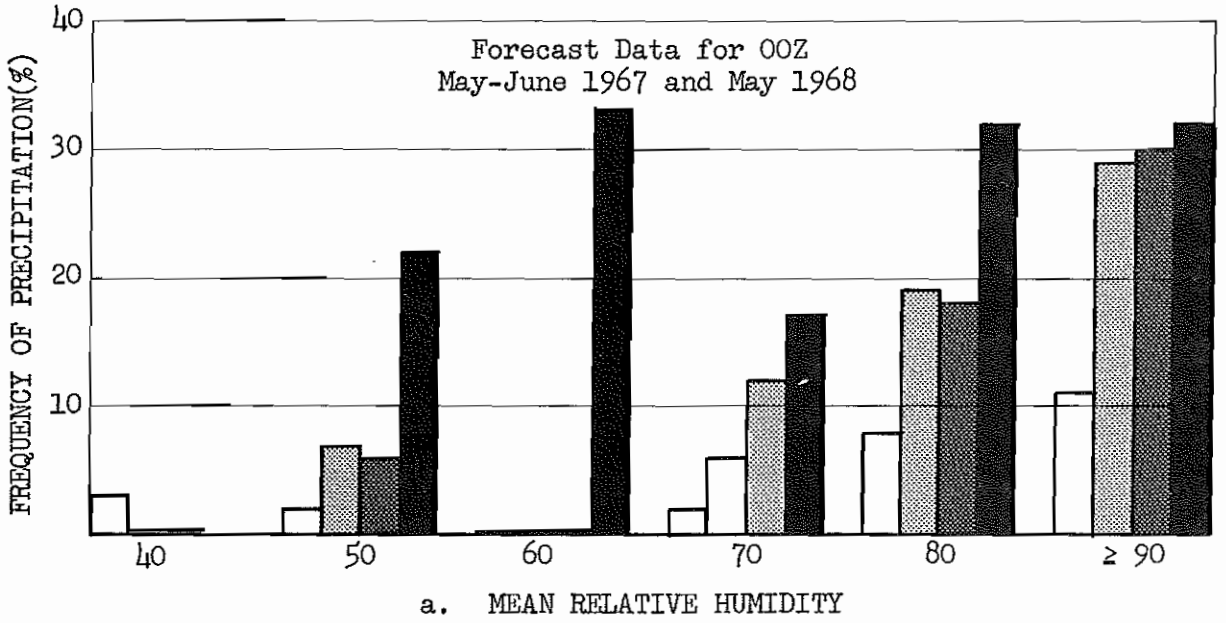

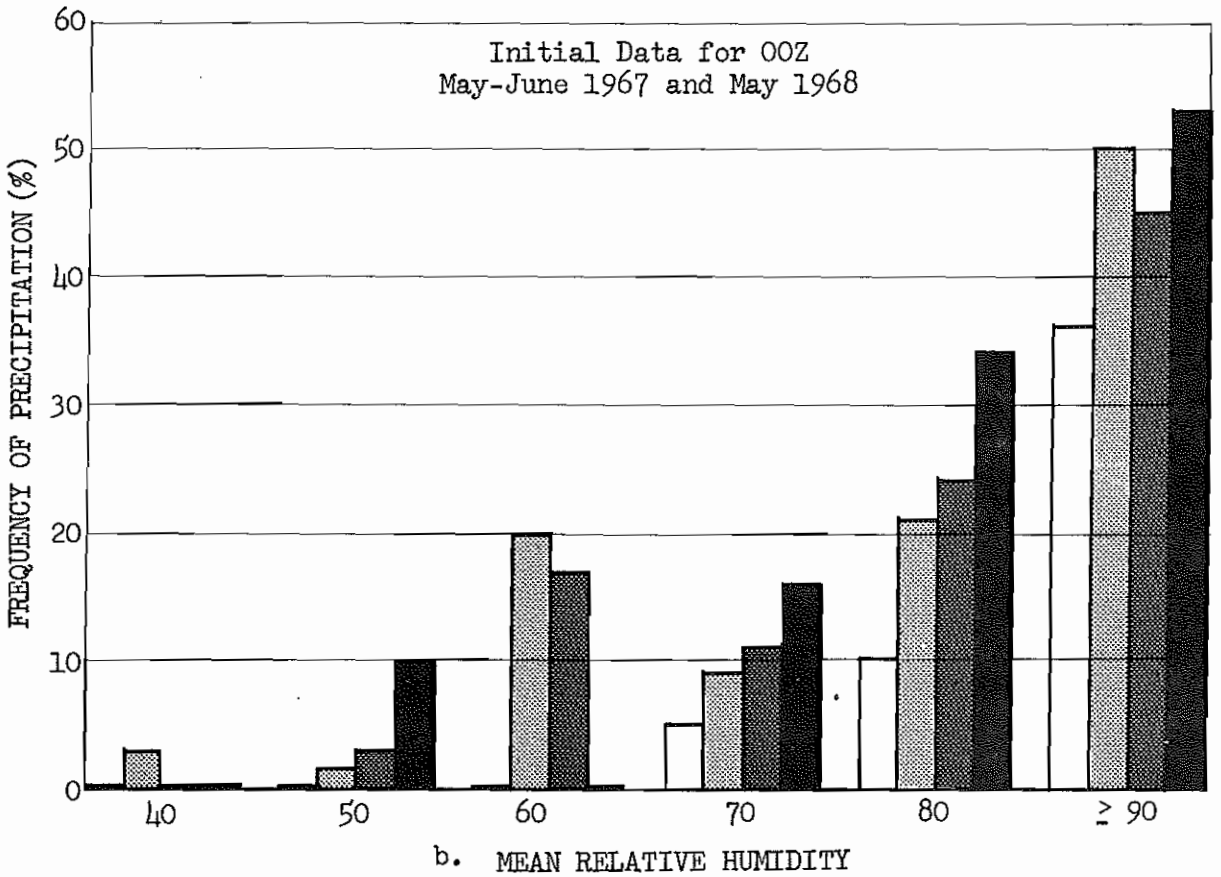

Key to Lifted Index classes

> + 3 | +3 to +1 | 0 to -3 | < -3

Figure 15

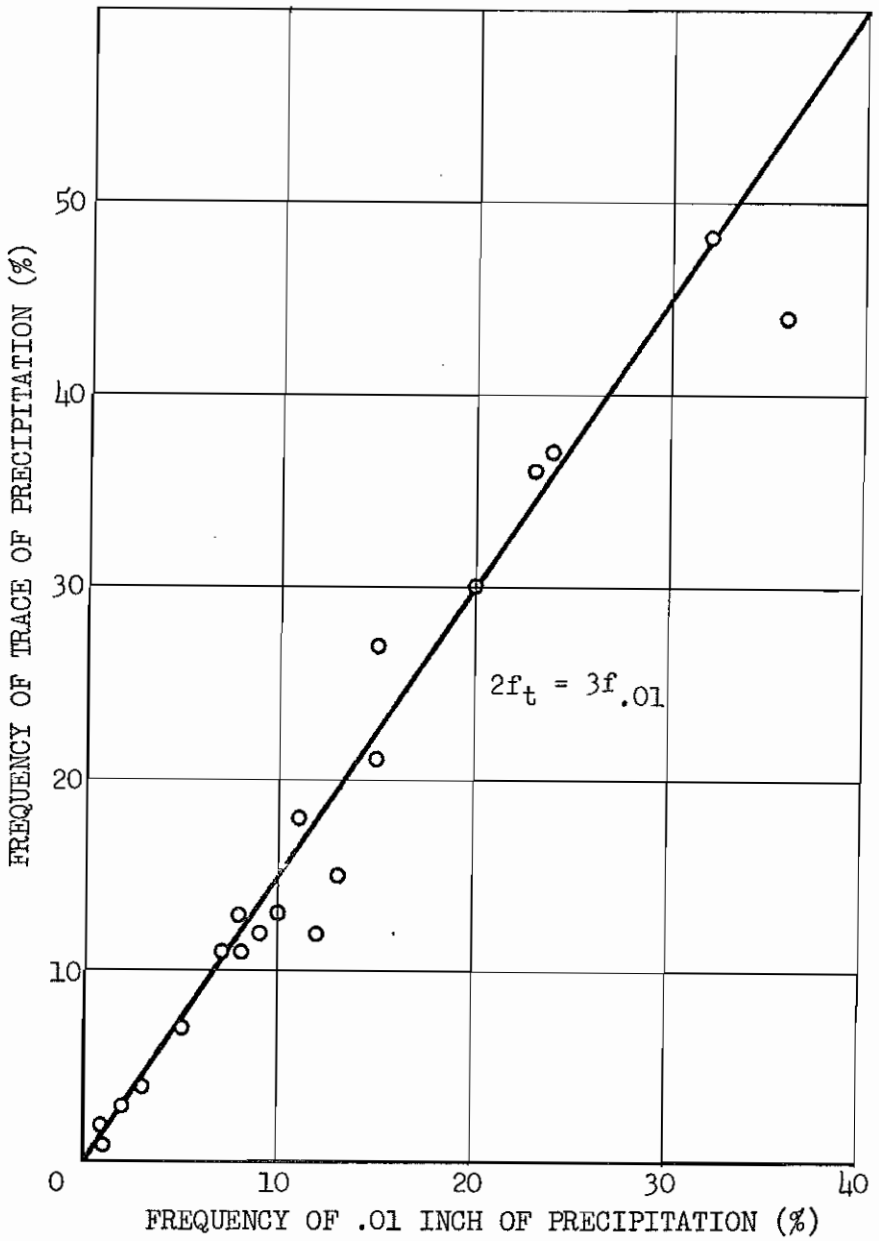

Figure 16

The tabulated data were analyzed on scatter diagram (Figure 16). For measurable precipitation probabilities less than 40%, visual inspection shows no large and consistent departures from the relationship:

$$2f_t = 3f_{.01}$$

where f_t is the frequency of a trace in 6 hours and $f_{.01}$ is the frequency of a measurable amount in a like period.

In the frequency range for which data are available, a trace is thus seen to occur about 1.5 times as often as amounts $\geq$.01 inch. Although this relationship might be expected to vary with weather regimes and with the probability of measurable amounts of precipitation, it can serve as a forecaster's rule of thumb, particularly for moderate and low probabilities.

COMBINING TWO 6-HOUR PRECIPITATION PROBABILITY VALUES INTO ONE 12-HOUR

If the 12-hour probability of .01 inch of precipitation is denoted by the letter C, and the two 6-hour probability values contained in the 12-hour period are represented by the letters A and B respectively, elementary probability states that

$$Pr(C) = Pr(A) + Pr(B) - Pr(AB)$$

The term Pr(AB) is defined as the probability of both A and B occurring and represents the degree of dependence between A and B. There obviously is dependence between the occurrence of rain in two adjacent 6-hour periods, but the dependence must be evaluated empirically.

Statistical data related to the persistency tendency of precipitation between 6-hour periods is available in ESSA Technical Report, WB-5, Climatological Probabilities of Precipitation for the conterminous United States, by Donald L. Jorgensen, December 1967.(17) Information there is presented in the form of monthly charts showing station 6- and 12-hourly climatological frequencies of measurable precipitation based on 15 years of data. A scatter diagram plotting of station 6-hour probabilities and corresponding 12-hour values yielded Figure 17 with the analysis fitting the data very well. Table 4 converts the graph into incremental 10% intervals.

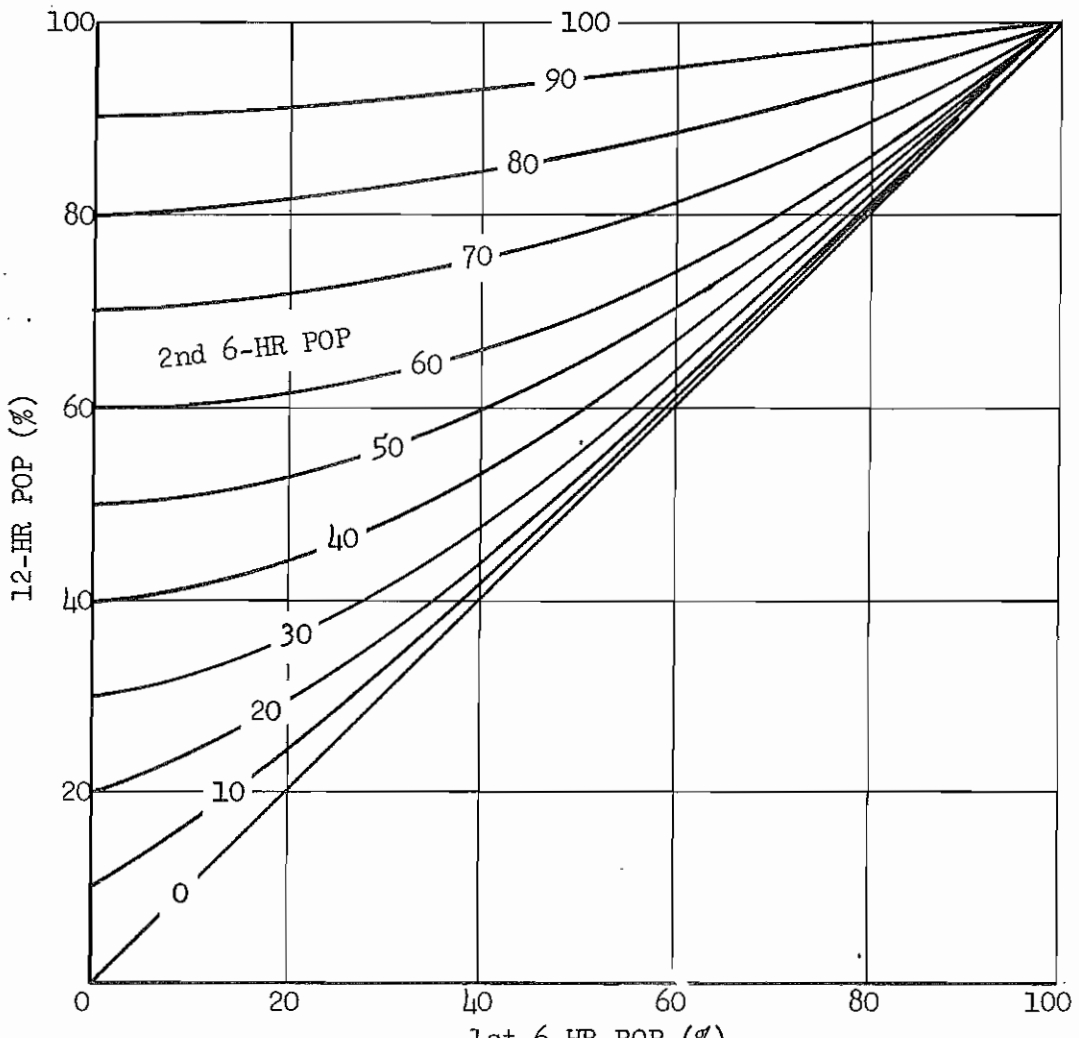

Figure 17

TABLE 4
12-Hour Probability of Precipitation
Based on Consecutive 6-Hour Values

6-Hour POP	6-Hr POP For Adjacent Period									
	10	20	30	40	50	60	70	80	90	100
10	16	23	32	41	51	61	71	81	90	100
20	23	30	36	44	52	62	72	82	91	100
30	32	36	40	47	55	64	73	83	92	100
40	41	44	47	53	59	67	75	84	93	100
50	51	52	55	59	64	70	77	86	94	100
60	61	62	64	67	70	74	79	88	95	100
70	71	72	73	75	77	79	83	90	96	100
80	81	82	83	84	86	88	90	93	97	100
90	90	91	92	93	94	95	96	97	99	100
100	100	100	100	100	100	100	100	100	100	100

A more rigorous definition of the relationship would come from analysis of a large number of individual cases if these data were available. A few characteristics of the family of curves, however, lend confidence to the reality of the graph. Data from various geographical areas were used in the plotting. For instance winter information from the Pacific Northwest was included along with some from Florida in summer months in order to define relations between high frequency values of differing meteorological regimes. Data from the arid Southwest were included also. No variation in data fit was noted on a geographical basis.

One will note that a very similar result obtains by substituting first period values for second 6-hour values and conversely. This resulted without forcing the data. For instance, 20% for the first period combined with 60% for the second gives 62% for twelve hours, and 60% for the first combined with 20% for the second also gives 62%.

Intuitively one knows that zero probability in one period combined with a certain value in an adjacent one equals that value for the combined period. This feature fixes the ordinate intercepts and the diagonal that limits the curves. Similarly, certainty (100%) for a period combined with any value for another results in 100% for the combined periods. This results in the curves converging in the upper right. Further, if the occurrence of precipitation in one 6-hour period were independent of its occurrence in the adjacent one it would be possible to multiply probabilities to obtain the AB term in the expression

$$Pr(C) = Pr(A) + Pr(B) - Pr(AB)$$

This hypothetical state of independence could be represented on the graph as a family of straight lines connecting the 12-hour POP values (left margin) and the upper right corner. These straight lines are a constraint, or limit, upon the shape of the empirical lines.

The graphical relation presented in Figure 17 is judged to be a good first approximation for the conversion of sequential 6-hourly probability values into the corresponding 12-hour probability.

THE RELATIONSHIP OF PE PARAMETERS TO CLOUDINESS

The forecasting of cloudiness is a major concern of both general and specialized meteorologists in the service programs of the Weather Bureau. Not only is it specified in the body of forecasts, but, it is a critical ingredient in forecasts of temperature, low level wind and turbulence, snow melt, visibility, and other weather elements. Cloudiness approaches being a common denominator for all forecasting activity, but subjective extrapolation for shorter periods and non-rigorous circulation models for longer periods are the common mainstays in cloudiness forecasting. Objective techniques for applying PE parameters to the cloudiness forecast problems should be most helpful.

The main thrust of the study of PE parameters was to help make objective the specification of the probability of measurable precipitation, but limited information on cloudiness was part of the data collection for the study. This consisted of listing for each of the 50 stations the value of total sky cover "N" from plotted 00Z and 12Z surface weather charts. In stratifying the data for study, two simple categories were established:

$$N \leq 4 \text{ and } N > 4$$

corresponding to scattered plus clear conditions on the one hand and broken, overcast, or sky obscured on the other. "N",of course, includes cirrus type cloudiness as well as middle and low clouds, and those of vertical development.

Precipitation occurrences are dichotomous, i. e., events fall into either a rain or no rain category. While values of Synoptic Code "N" range from 0 to 9, the stratification selected results in two categories that may be called "cloudy" or "not cloudy". Another comparative feature is noteworthy. While the frequency (climatological probability) of measurable precipitation in 6-hours for the entire data sample was 0.10, the comparable frequency of "cloudy" at 00Z and 12Z was 52%. Thus to be really useful to forecasters, the probability specifying ability of PE parameters for "cloudy" weather should be considerably greater than for precipitation.

Figure 18a compares for $\overline{RH}$ categories the effect of considering or not considering $VV \geq +1$. The salient point shown is that $\overline{RH}$ stratifications give frequencies of "cloudy" ranging from 16% for low humidity to over 90% for near saturation - indicating good resolution, or discrimination, from the sample climatology (51% for the data displayed). Beyond this, consideration of the selected VV classes permits further resolution of about 10% probability when $\overline{RH}$ ranges from 50% to 80%. The graph of 24-hour forecasted VV and $\overline{RH}$ values (Fig. 18b) exhibits only slightly less effectiveness for forecasts than for initial data.

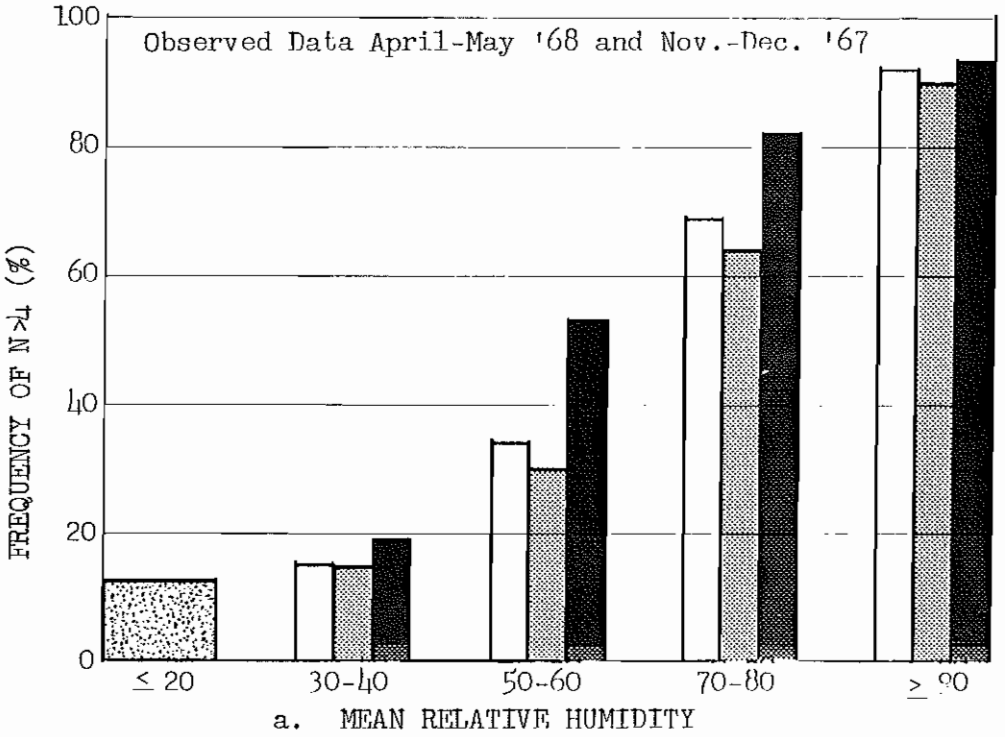

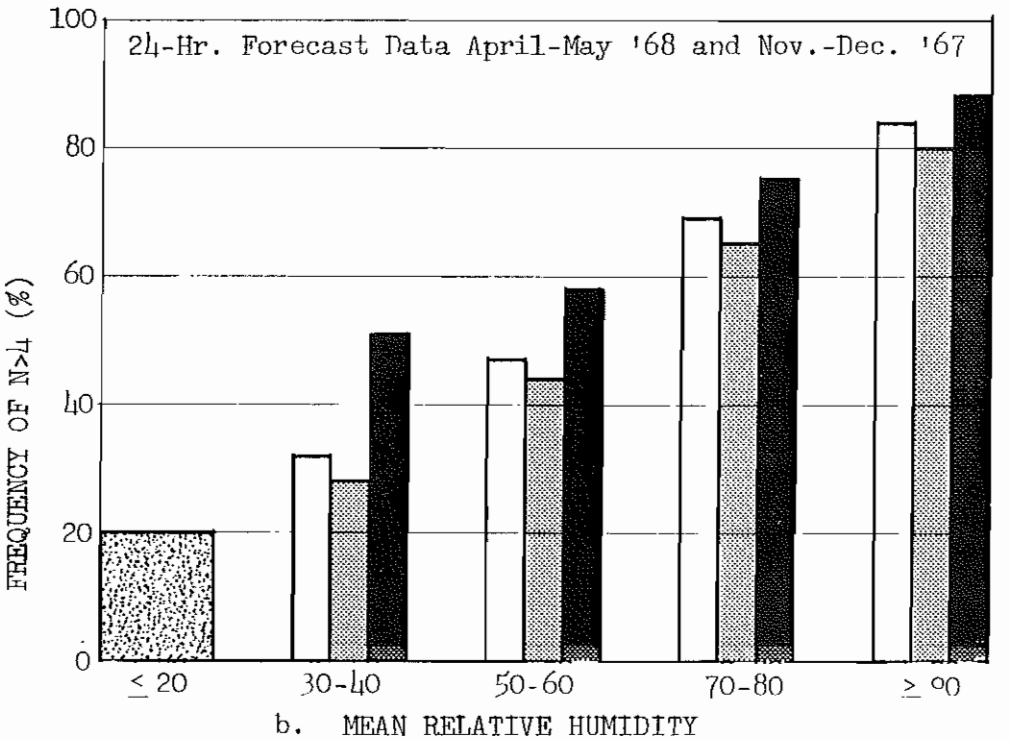

Figure 18

Sample size precludes break-down | Irrespective of VV | VV<+1 | VV≥+1

The array of frequency of "cloudy" vs classes of Lifted Index within $\overline{RH}$ categories (Figure 19a) shows a positive correlation of instability and cloudiness at $\overline{RH}$ values below 90%. In the most moist category, Lifted Index appears to add nothing to information already contained in $\overline{RH}$ and this conclusion is confirmed in the forecast data presented in Figure 19b. In comparing forecast with initial conditions one finds the usual moderate deterioration with time in specifying ability of both $\overline{RH}$ and LI.

In view of the variations in the effects of VV and LI on precipitation from early morning to afternoon conditions, a comparison was made of the effect of these parameters on cloudiness at 00Z and 12Z for a warm season sample. VV initial data is shown in Figures 20a and 21a. The characteristic of VV being most effective in the $\overline{RH}$ range 50% to 80% irrespective of time of day (Figure 18a) shows in both 00Z and 12Z graphs. In this range "upward motion" is more pronounced in producing "cloudy" at 12Z than at 00Z, paralleling the findings with respect to precipitation. Untoward results are shown at extreme $\overline{RH}$ ranges - partially due to the small number of cases in the categories. Some of the seemingly unreasonable features disappear in the 24-hour forecasts of VV (Figures 20b and 21b), agreeing with other recognitions that 24-hour forecast VV values relate better to weather occurrences than do initial (6-hour forecast) values. For the forecast data, VV appears to contribute slightly more to cloudiness specification at 12Z than at 00Z but this is not marked, and an unqualified conclusion to this effect is not warranted due to the size of the sample. It was judged proper to omit May-June '67 data from the analysis of vertical velocity effects on cloudiness because the PE model produced unrepresentative vertical velocity patterns during that period.

May-June '67 LI data were combined with April-May '68 information to study the diurnal, warm season Lifted Index relationship to "cloudy" weather (Figures 22 and 23). There is shown an overall stair-stepping of the LI class bars within $\overline{RH}$ categories indicating a positive correlation of cloudiness frequency with instability. The $\geq$ 90% $\overline{RH}$ is a notable exception, the implication being that relatively high moisture is a sufficient criterion for high probability of "cloudy" weather, but with the added information that this holds irrespective of time of day. No contrasting features between 00Z and 12Z data were discerned that would be of significant advantage to forecasting.

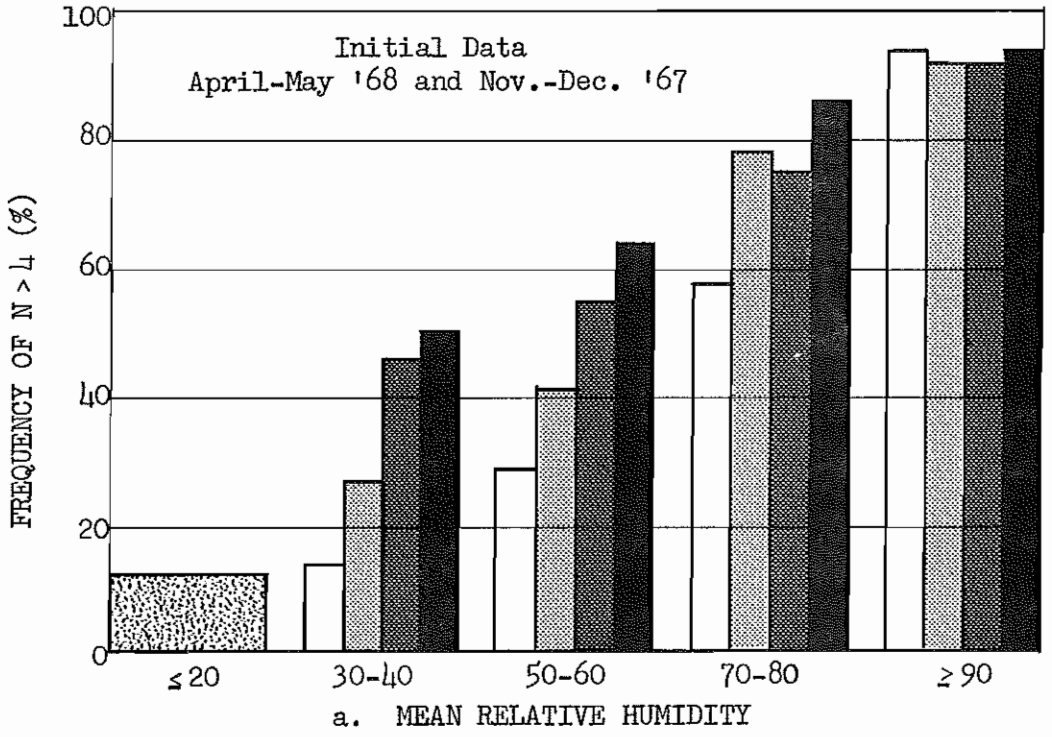

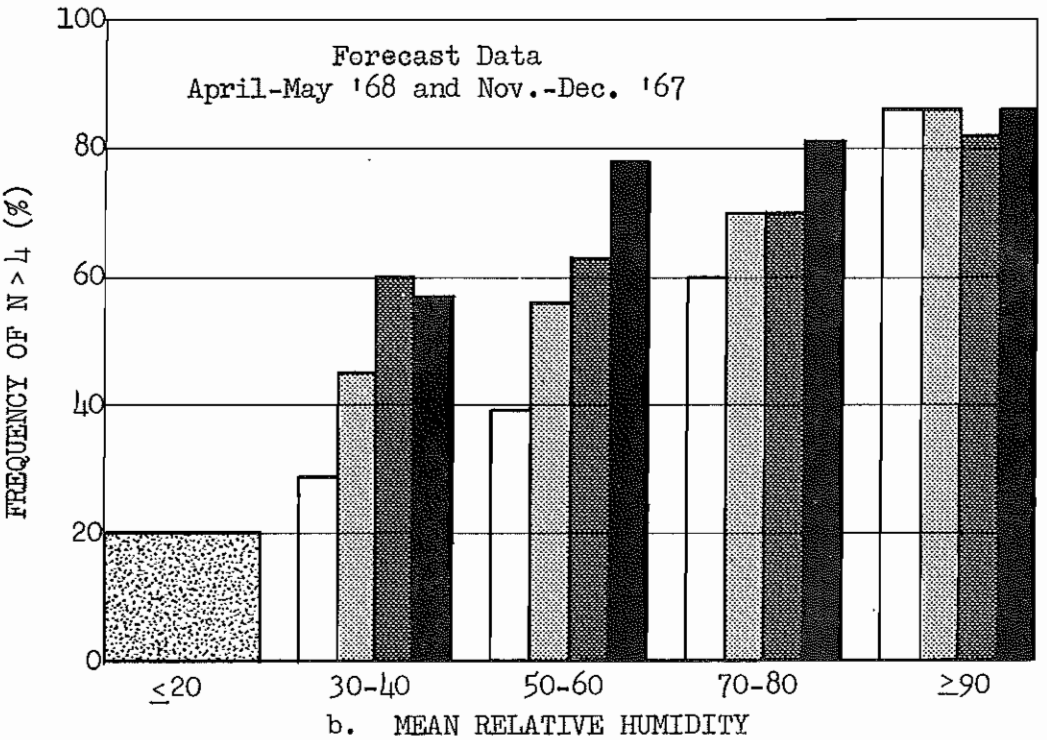

Key to Lifted Index classes

Sample size precludes break-down | >+3 | +3 to +1 | 0 to -3 | <-3

Figure 19

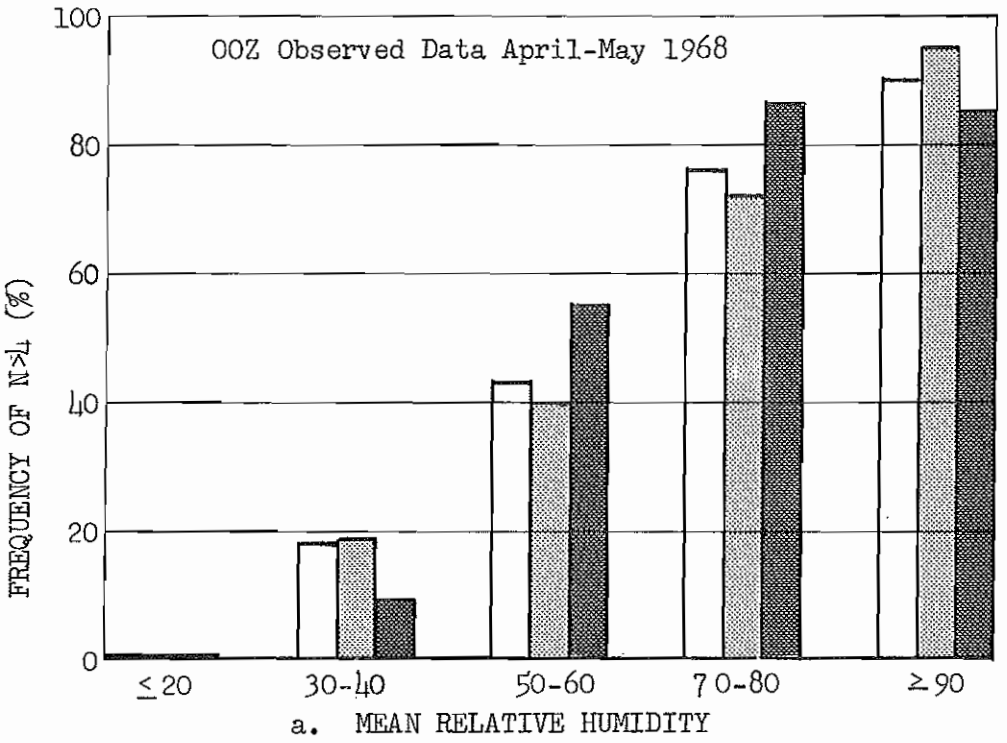

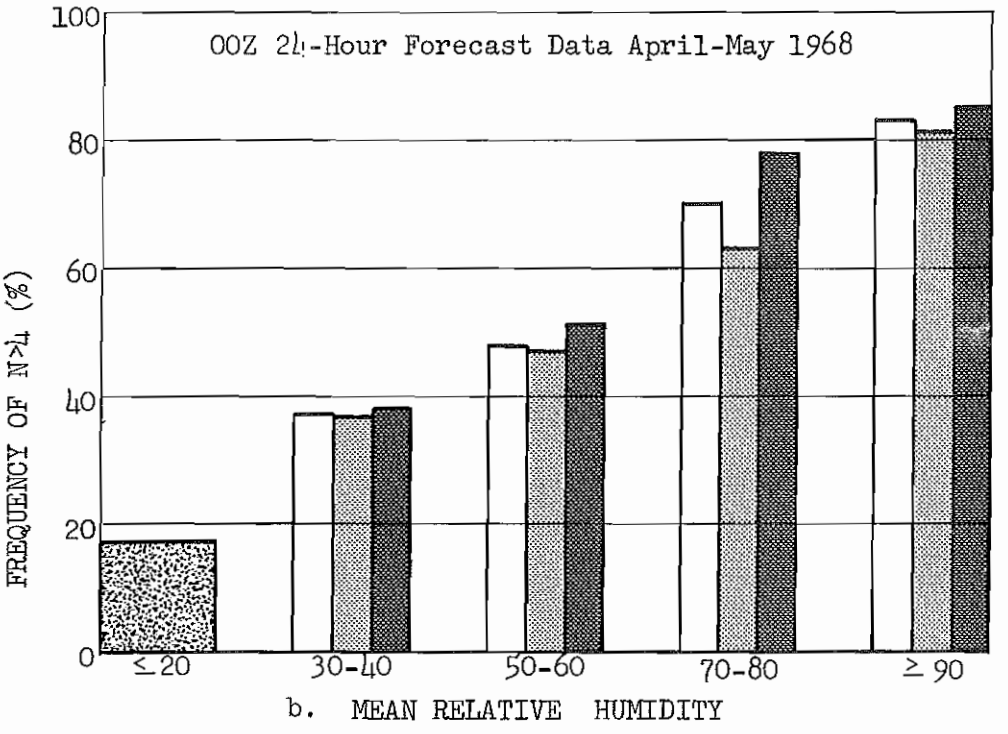

Figure 20

Sample size precludes break-down
Irrespective of VV
VV<+1
VV≥+1

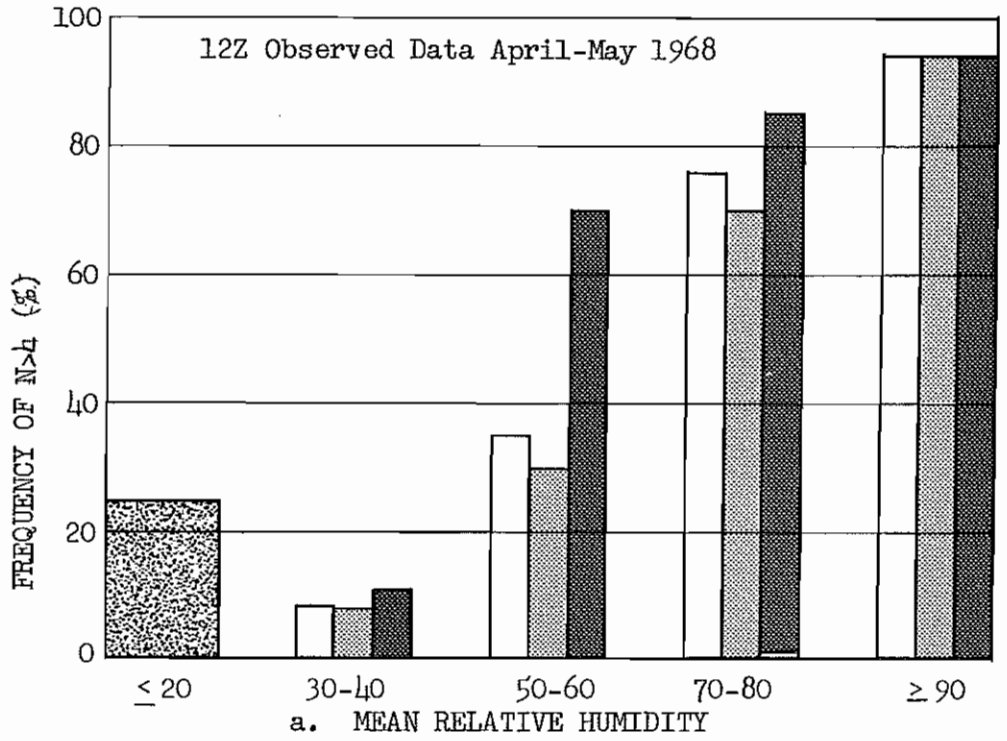

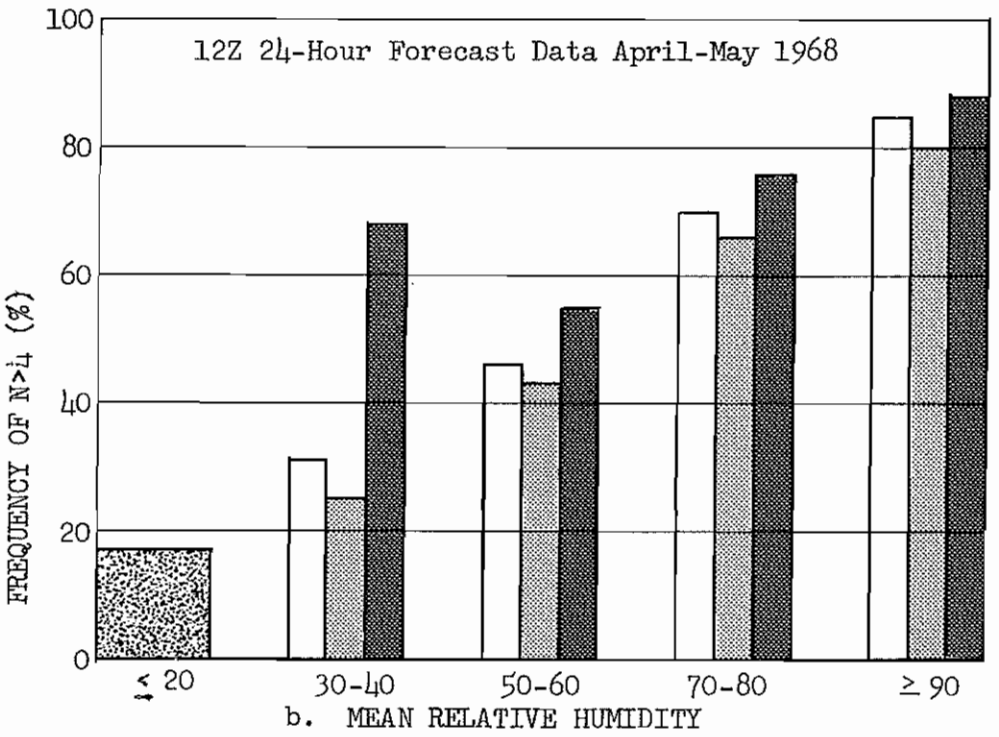

Sample size precludes break-down

Irrespective of VV

VV<+1

VV≥+1

Figure 21

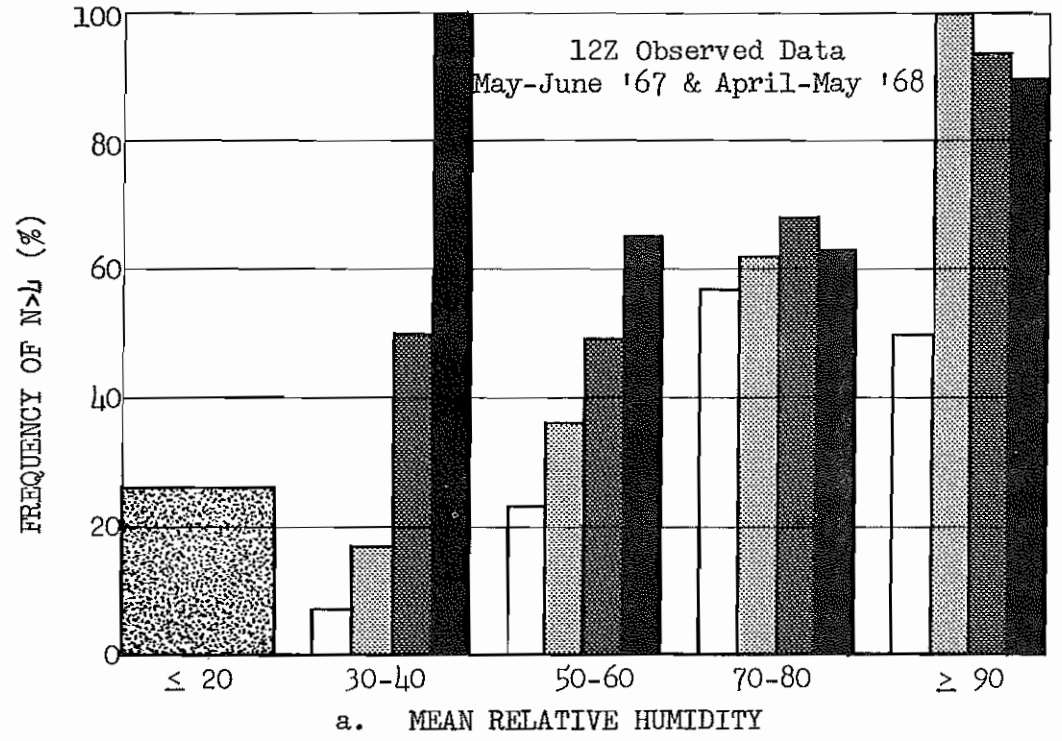

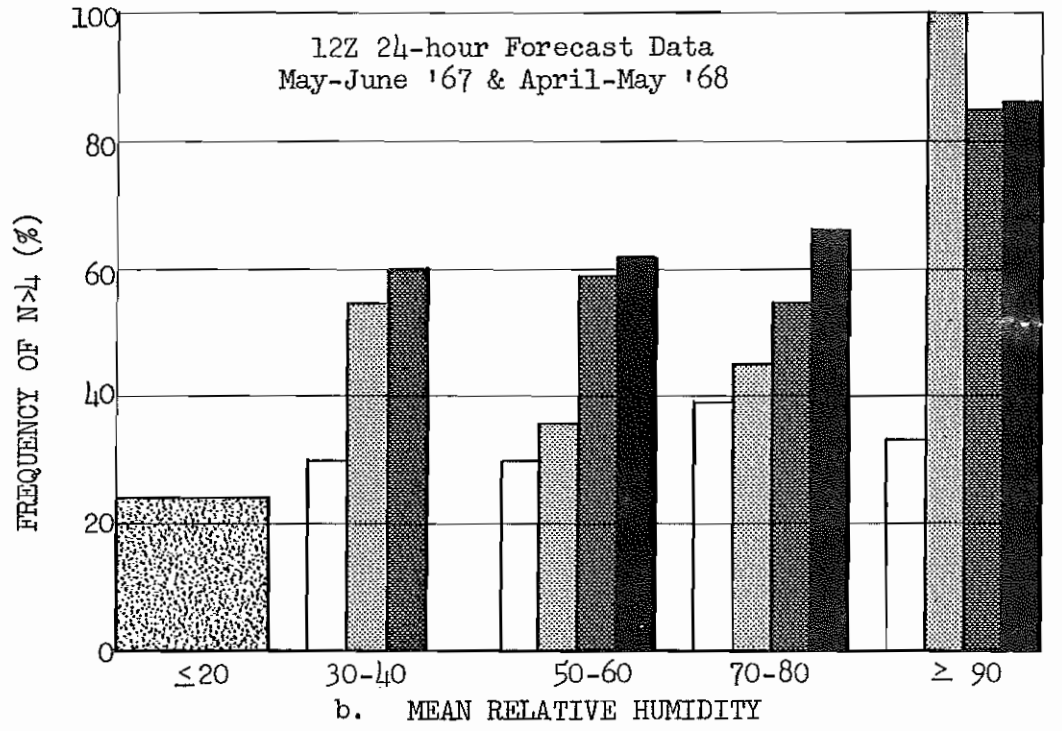

Key to Lifted Index classes

Sample size precludes break-down | >+3 | +3 to +1 | 0 to -3 | <-3

Figure 22

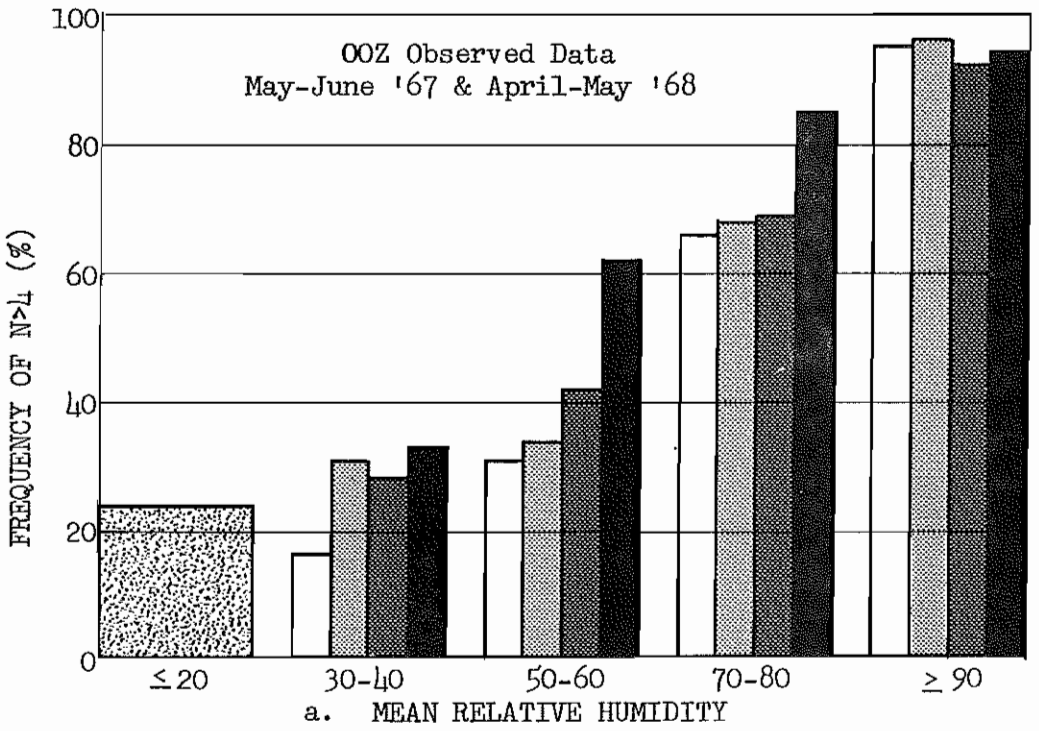

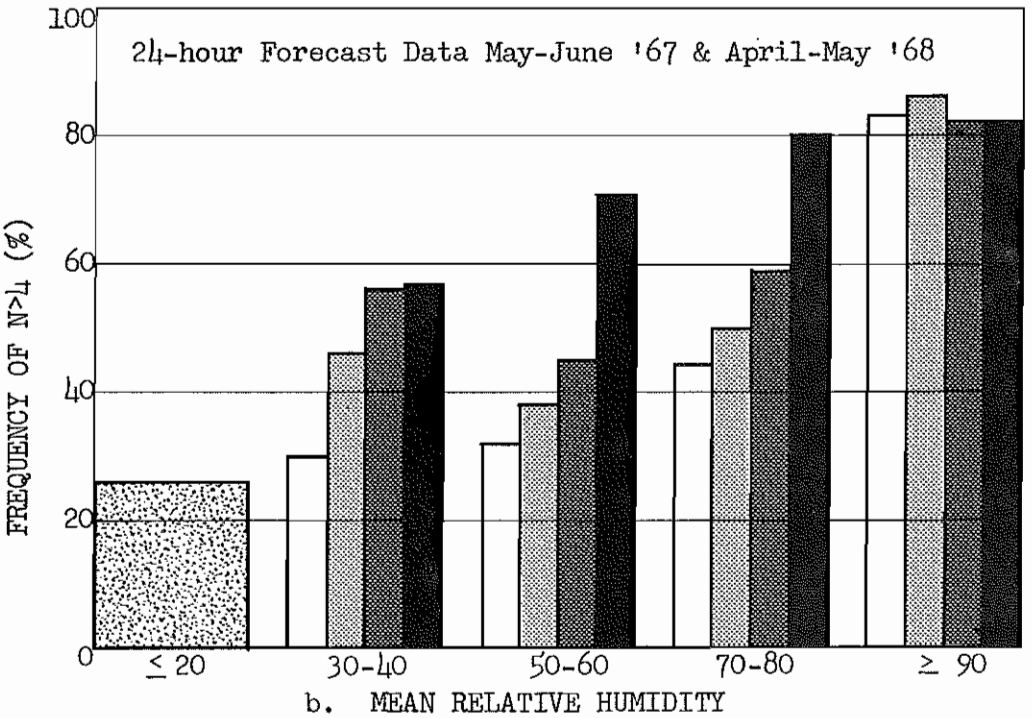

Key to Lifted Index classes

Sample size precludes break-down | >+3 | +3 to +1 | 0 to -3 | <-3

Figure 23

USE OF PREDICTORS IN FORECASTING ROUTINES

Forecasters have a requirement to time precipitation events as closely as possible and are interested in precipitation probabilities for 6-hour or shorter periods. There is also a need, as in public forecasts for "tonight" or "tomorrow", for an expression of 12-hour precipitation probability. Therefore, this study has included the development of relationships between predictors routinely available in the PE model output and six-hour precipitation probability plus an aid, discussed on page 21, for use in obtaining an estimate of the 12-hour probability from two successive 6-hour estimates.

The precipitation amounts considered were for the six hours prior to the 00Z and 12Z valid times of the PE parameters. However, the procedure outlined below is recommended for extending the probability estimates to any period for which values of the PE predictors are available. PE forecast data for 6-hourly intervals have been transmitted on teletype for trial use at certain stations but, at least for the present, facsimile charts will need to be used, with interpolation for the time and specific location.

Facsimile presentations of the fields of $\overline{RH}$, VV, and LI are available before 09Z and 21Z daily. Thus, forecasts from 00Z data are received in time to apply to the "today" and "tonight" portion of 10Z forecast issuances and forecasts based on 12Z data are available for use in the "tonight" and "tomorrow" portion of 22Z issuances. The fax-panel PE data for 00Z and 12Z can be supplemented by interpolated values for 06Z and 18Z. The following diagram illustrates the suggested schedule for use of the PE data and the relationships developed in the study:

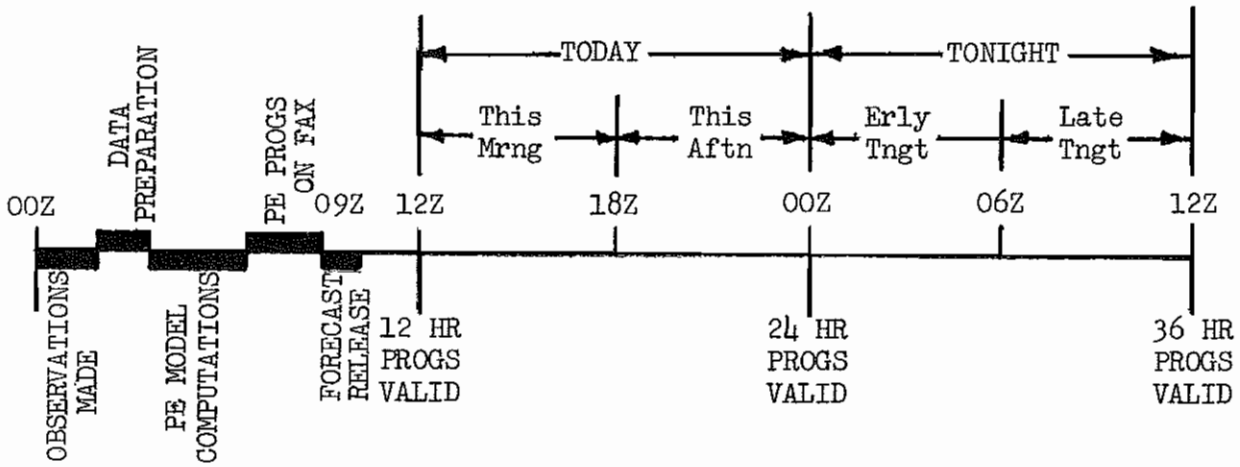

Applicable Relationships. As discussed earlier, $\overline{RH}$ and VV were found to be the most satisfactory predictors for the cooler season; the independent effect of LI could not be determined. Therefore during the season October-April Figure 26 is to be used for successive 6-hour periods, and the increments combined using Figure 18 (or Table 3).

From May through September two graphs are applicable in the forecast routine. Figure 24, relating precipitation probability to the combined effect of $\overline{RH}$ and VV is to be used for the 6-hour periods ending at 12Z and 18Z; Figure 25, representing the influence of $\overline{RH}$ and LI in combination, is to be used for the 6-hour periods ending at 00Z and 06Z.

As an example, applicable data available for San Antonio, Texas at 21Z on September 24, 1968 was:

		← Tonight* →		← Tomorrow* →	
Date/Time	25/00Z	(25/06Z)	25/12Z	(25/18Z)	26/00Z
Forecast	12-hr	(18-hr)	24-hr	(30-hr)	36-hr
$\overline{RH}$	90	(93)	97	(98)	92
VV	0	(+1)	+1	(0)	0
LI	-4	(-4)	-4	(-4)	-4

( ) indicate interpolations between chart panel times
* Probabilities based on predictor values at end of 6-hour periods

Using Figure 25 with the 25/06Z values of 93% for $\overline{RH}$ and -4 for LI, a probability of 51% is obtained for the 25/00Z - 25/06Z period. For the subsequent six hours, Figure 24 is used with 25/12Z values of 97% $\overline{RH}$ and +1 VV to yield an estimate of 34% probability. The probability figures of 51% and 34% can then be used in conjunction with Table 3 or Figure 18 to provide an estimate of 58% probability for the 12-hour "Tonight" period, 25/00Z to 25/12Z. The forecast for "Tomorrow" can be obtained in an analogous manner.

By use of the relationship $2f_t = 3f_{.01}$, discussed on page 17, the forecaster can supplement the estimate of probability of a measurable amount for a 6-hour period by obtaining an indication of the likelihood of a trace, which may at times be helpful information.

Cloudiness Forecasts. The relationships of the PE parameters to cloudiness discussed in the section beginning on page 23, can be applied in the forecasting routine. Although forecasts of sky condition are not usually expressed in probabilistic terms, consideration of the frequency distributions in Figures 19-21 can give the forecaster an estimate of the probability of "cloudy" conditions and add to the confidence in his categorical forecasts. Forecasts of $\overline{RH}$ and VV

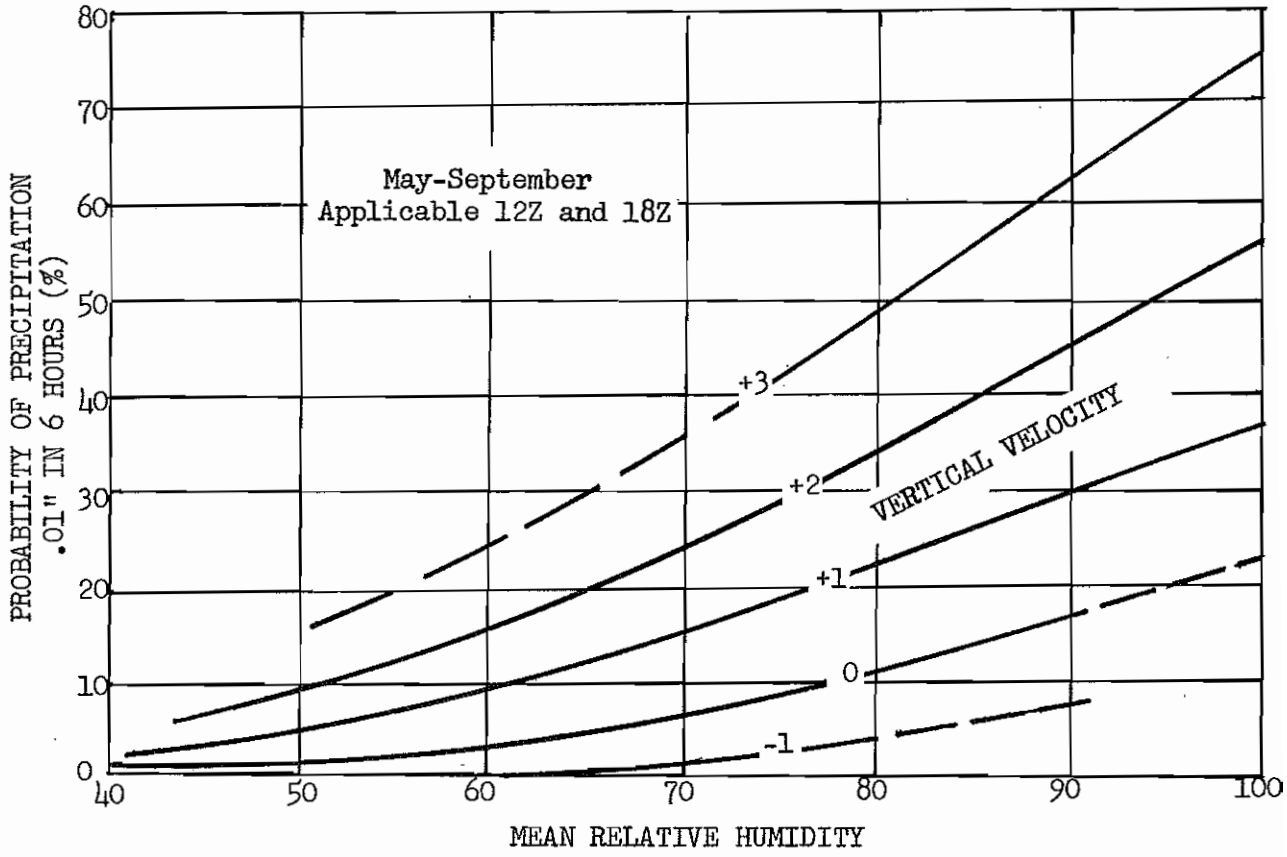

Figure 24

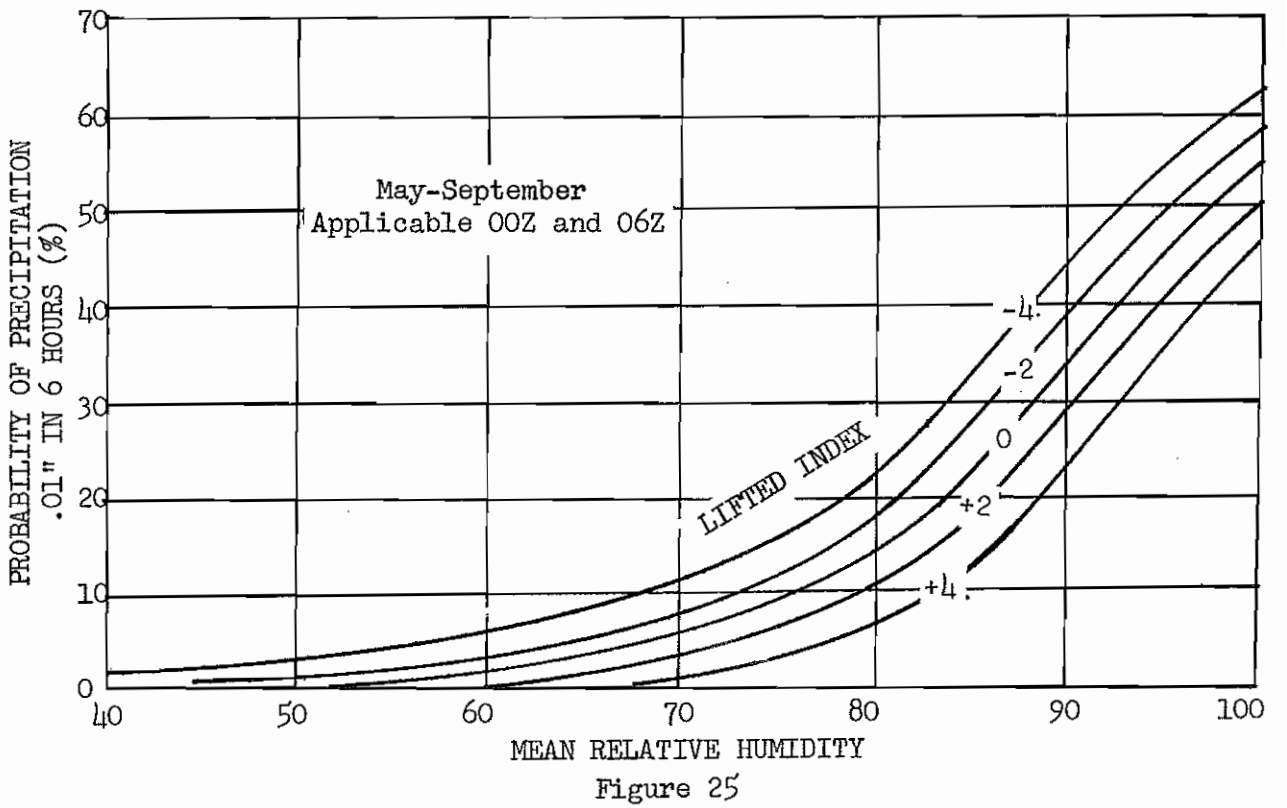

Figure 25

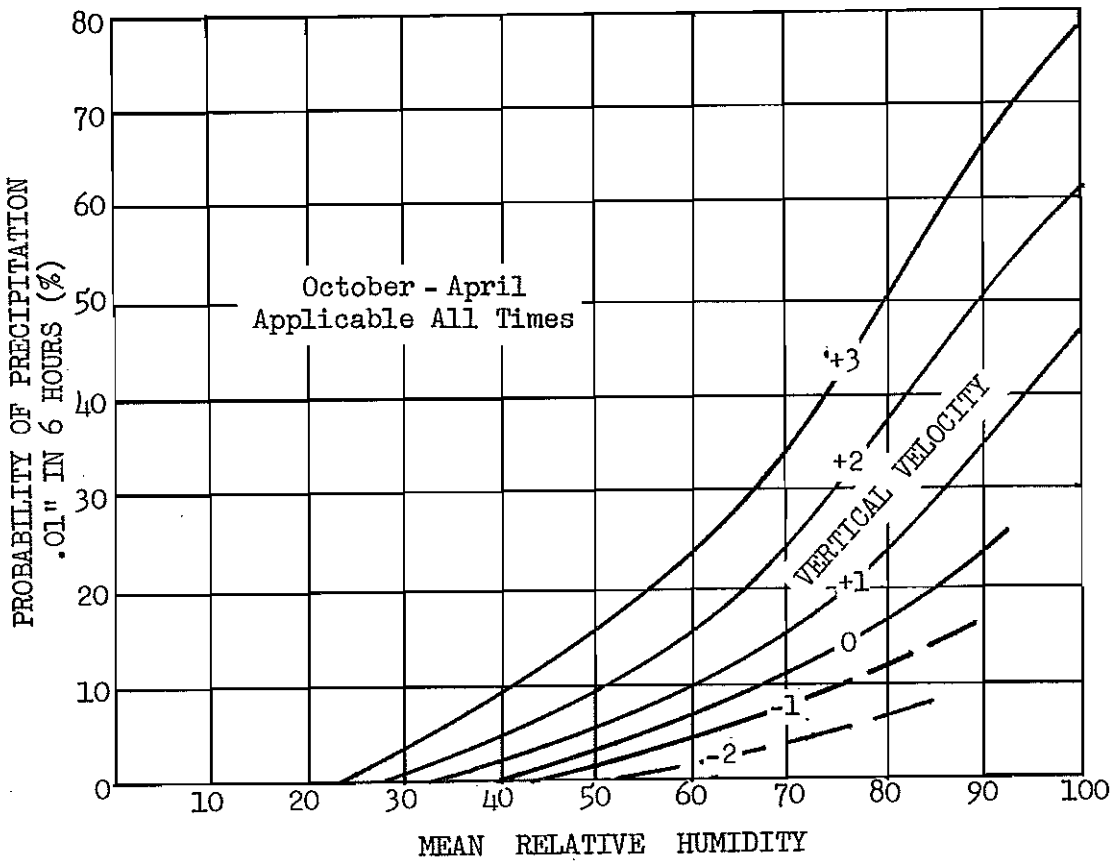

Figure 26

show good specifying ability for cloudiness and, considering that only slight skill is added by a diurnal break-down or consideration of LI, Figure 19b is the recommended aid in forecasting cloudiness.

Use of the Sub-synoptic Advective Model (SAM). A discussion of some applications of the SAM forecasts to probability forecasts is included as an Annex to this memorandum to serve as a convenient reference. Since the area covered by SAM forecasts extends only from the Mississippi to the U.S. east coast, the aids developed for use with SAM data are not applicable to all of the area (Figure 1) considered in the PE parameter study. However, for the stations for which the SAM teletype bulletins are available, the forecasts of Saturation Thickness Deficit and the graphs in the Annex may be used to obtain estimates of cloudiness and precipitation probabilities.

The SAM forecasts are transmitted over the RAWARC teletype system at approximately 0815Z and 2015Z and are applicable to 12 hour periods beginning at 12Z and 00Z. Since the forecasts are for three-hourly intervals, they can provide detail not obtainable from the techniques discussed for use with the PE predictors. The procedure for applying the information included in the Annex will be self-evident from the graphs and the discussions.

Reliability of Results. Most of the data accumulated for this study were used in developing the relationships which have been presented and cannot be applied to independent testing. Limited testing was carried out using independent data from June 1968. The sample included 511 spot forecasts for stations in the Weather Bureau Southern Region. The area east of the Mississippi was used in order that a comparison of SAM forecasts could be included. Forecasts were made for the standard "first" period of public forecasts - "today", or "tonight" - following the procedures outlined in this memorandum. Brier Scores were computed for forecasts based on the PE graphs and on the SAM relationships. These were compared with the scores for the official local forecasts for the same periods. Scores (a low figure is desirable) were:

"PE"	.132
"SAM"	.142
"LCL"	.131

Although no extensive testing has been possible, the relationships developed have been physically reasonable and it is believed that they will be fairly stable. At the very least, they will provide the forecaster with a convenient and systematic means of using the PE data in probability precipitation forecasts. As is usually the case, it is expected that the man-machine mix will result in the best forecast and that indications from procedures outlined here can serve as a base upon which the forecaster can build by using more subjective methods.

ANNEX

PROBABILITY FORECASTING FROM THE SUB-SYNOPTIC ADVECTIVE MODEL

The Sub-synoptic Advective Model (SAM) uses information from the PE model output, updated with hourly surface data, to provide forecasts of low-level circulation and a moisture parameter, Saturation Thickness Deficit, for most of the United States east of the Mississippi. SAM is discussed in references (5) and (18)

The curves displayed in Figure 27 can serve as an aid in assessing the likelihood of cloudy conditions, instantaneous precipitation, or the accumulation of .01 inch or more precipitation in a 3-hour period, based on the SAM forecast of Saturation Thickness Deficit (S_d). Curve (1) is for instantaneous precipitation (as reported in hourly aviation observations) at the end of the three-hourly S_d accumulation period. Curve (2) is a comparable relationship for .01 inch of precipitation during the three hours. The third curve relates S_d to cloudiness with "Fair" defined as clear, scattered clouds, or clouds above 20,000 feet. "Cloudy" includes all other conditions.

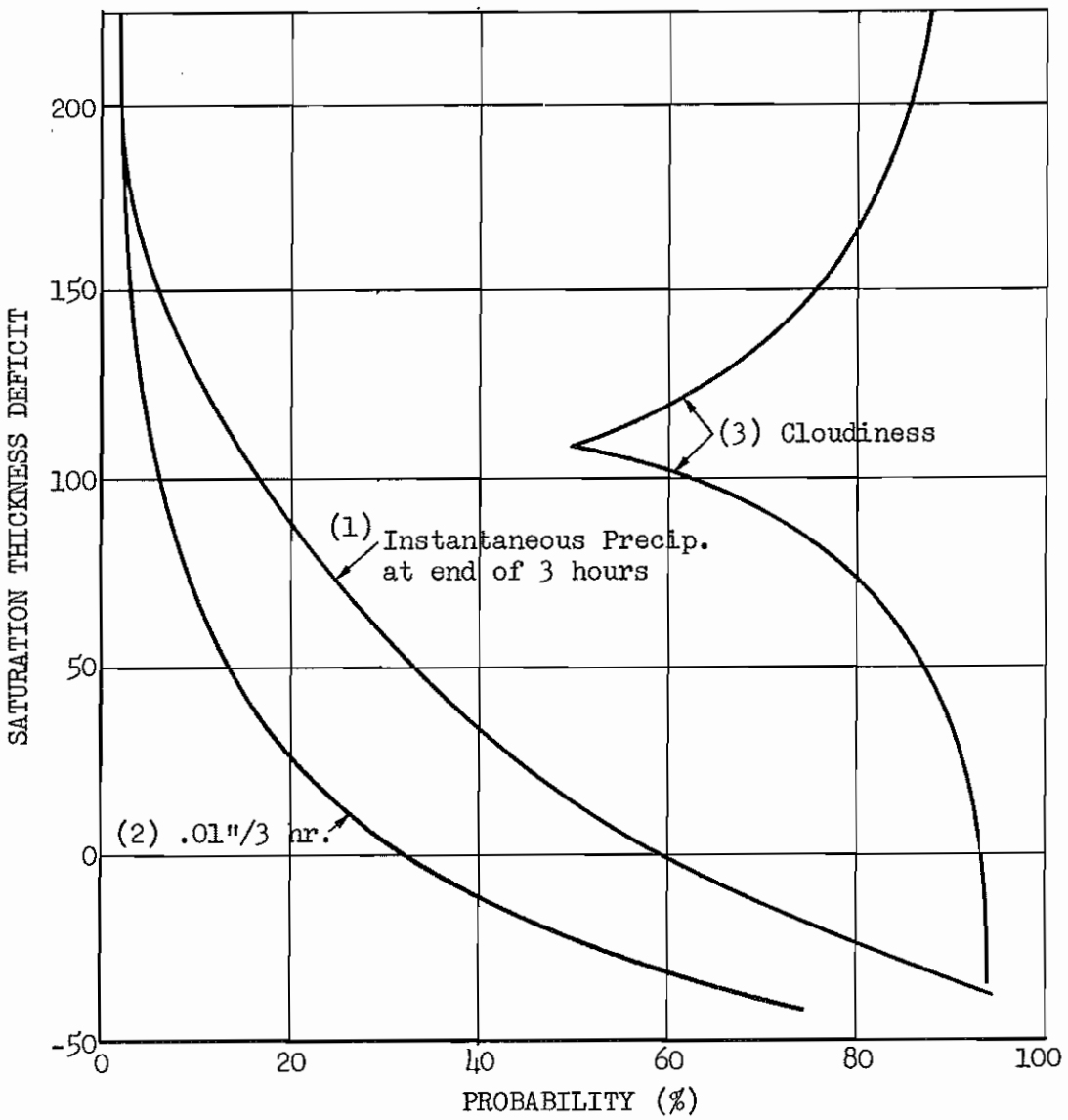

Figure 27

The first and third curves resulted from a study of data from the Weather Bureau Southern Region by Scientific Services. The second, from data in the North Central States, was developed by Scientific Services Division of Central Region Headquarters (18).

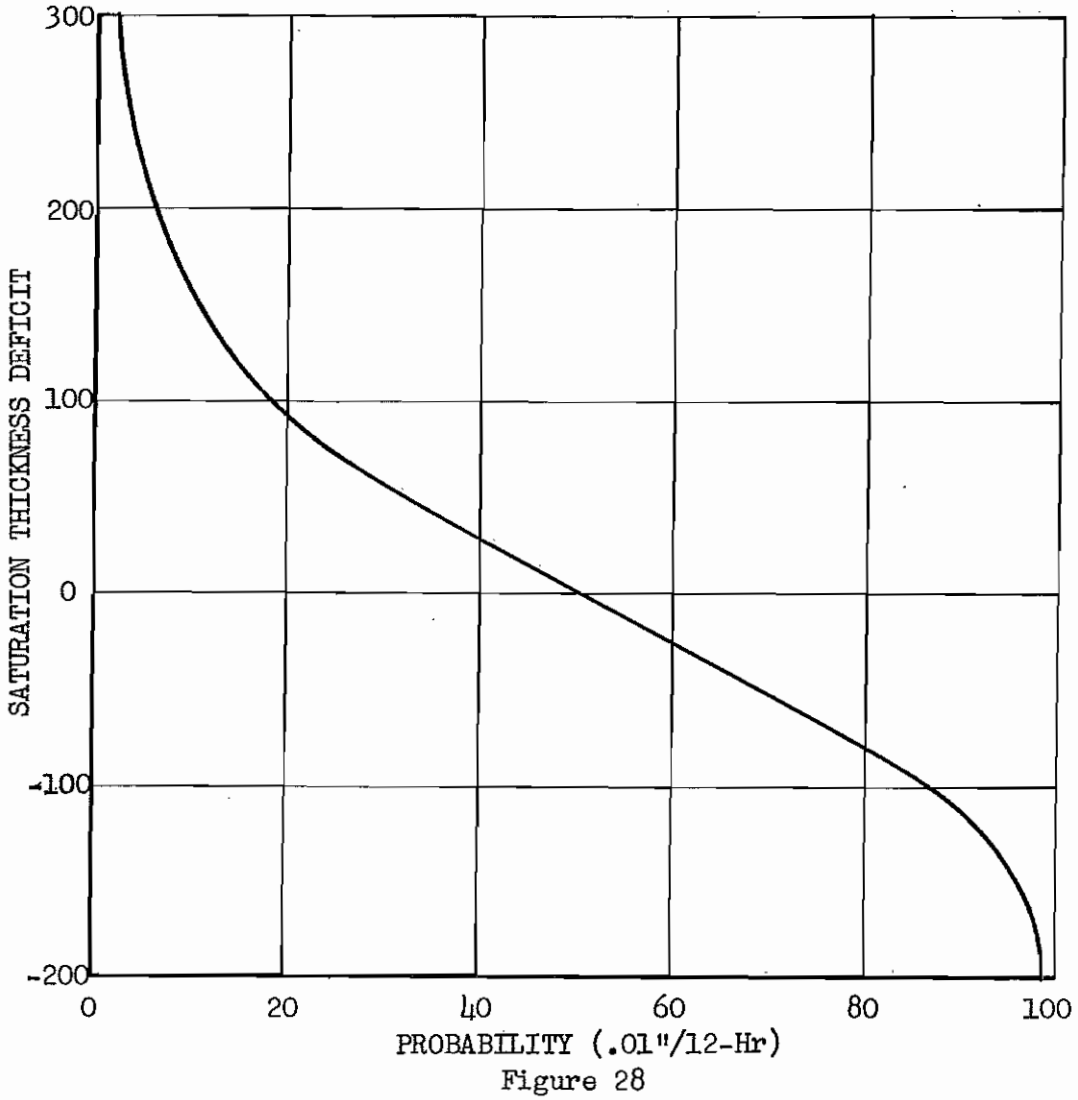

Figure 28

In public forecasting, the likelihood of .01 inch of precipitation in 12 hours is subject to verification, and forecasters in general have a keen interest in this event. Figure 28, also developed by Central Region Headquarters (18), relates S_d to .01 in./12 hours. The Saturation Thickness Deficit for 12-hours applicable to the graph is accumulated in this way: If all 3-hourly values are positive, the average of the four is taken; but if one or more negative values are present in the station 12-hour series, the negative values are summed disregarding positive values.

Work on specifying probability of precipitation from S_d is continuing in the Techniques Development Laboratory of the Bureau using a regression equation approach. Thus the exploratory work which culminated in Figures 27 and 28 is being expanded to a much greater sample which permits weighting of incremental 3-hourly S_d values.

Acknowledgment: Paul Moore and Jeter Pruett were the authors of the study. Computer programming to stratify the data was done by John Thomas and Jack Teague. Jerry Nunn and Linnie Frazier performed many analysis details and Larry Donahue extracted the data from facsimile charts. Most of the final drafting was done by Bob McNinch and the typing by Mrs. Frazier.

REFERENCES

(For abbreviations see note at end of references)

(1) Shuman, Frederick G. and Hovermale, John B.: An Operational Six-Layer Primitive Equation Model. JAM, Aug. 1968, 525-553

(2) ESSA-WB: UP-2, Four-Panel NWP Baroclinic Prognosis. WBFH No. 1, 6-5, Rev. 7/1/68

(3) ESSA-WB: SP-1, NWP Surface Prognosis. WBFH No. 1, 5-1, Rev.7/1/68

(4) ESSA-WB: SP-5, Prognosis of Probability of 0.01" Precipitation in 12 Hours. WBFH No. 1, 5-23, 10/1/67

(5) Glahn, H. R. and Lowry, D.A.: Short Range, Subsynoptic Surface Weather Prediction. WBTM TDL-11, July 1967

(6) ESSA-WB: Summary of Changes to PE Model. Staff Notes of Western Region, 6/11/68

(7) ESSA-WB: External and Internal Heat Sources and Sinks in the 6-Layer (Primitive Equation) Numerical Prediction Model. TPB No. 2, July 1967

(8) ESSA-WB: Saturation Criterion for Precipitation Forecasts in 6-Layer (PE) Numerical Prediction Model. TPB No. 3, July 1967

(9) ESSA-WB: Change in Representation of the Mean Relative Humidity Charts. TPB No. 4, Aug. 8, 1967

(10) ESSA-WB: Initial Moisture Analysis in the 6-Layer (PE) Numerical Prediction Model. TPB No. 5, Aug. 9, 1967; Addendum distributed with TPB No. 9, dated Jan. 18, 1968

(11) ESSA-WB: Sea-Level Pressure Forecasts from 6-Layer (PE) Numerical Prediction Model. TPB No. 7, September 13, 1967

(12) ESSA-WB: Lapse Rate Checking Procedures in the 6-Layer (PE) Numerical Prediction Model. TPB No. 9, Jan. 18, 1968

(13) ESSA-WB: Precipitation Forecasting in the 6-Layer (PE) Numerical Prediction Model. TPB No. 12, March 13, 1968

(14) ESSA-WB: Divergent Initialization of the 6-Layer (PE) Numerical Prediction Model. TPB No. 13, May 13, 1968

(15) ESSA-WB: Surface Topography Used in the 6-Layer (PE) Numerical Prediction Model. TPB No. 15, August 2, 1968

REFERENCES (Cont.)

(16) Harned, Stephen: The Lifted Stability Index and Associated Probabilities of Thundershower Occurrence at Tri-City. Manuscript Local Forecast Study, WBAS, Bristol, Tennessee, August 1968

(17) Jorgenson, Donald L.: Climatological Probabilities of Precipitation for the Conterminous United States. ESSA Technical Report, WB-5, December 1967

(18) ESSA-WB: SAM Verification Results. Central Region Headquarters Staff Notes, April 1968

Abbreviations used in the list of references:

JAM: Journal of Applied Meteorology, American Meteorological Society

WBFH No. 1: Weather Bureau Forecasters Handbook, Volume 1

WBTM: Weather Bureau Technical Memorandum

TDL: Techniques Development Laboratory, Systems Development Office, Weather Bureau Central Headquarters

TPB: Technical Procedures Bulletin, numbered serially, produced by Technical Procedures Branch, Weather Analysis and Prediction Division, Office of Meteorological Operations, Weather Bureau Central Headquarters in collobration with the National Meteorological Center, Suitland, Maryland

SAM: Sub-synoptic Advective Model

UP-: Upper Air Prognosis

SP-: Surface Prognosis

LIST OF SOUTHERN REGION TECHNICAL MEMORANDA

No. 1 Selection of Map Base for Small Scale Analysis and Prediction. Woodrow W. Dickey - May 19, 1965

No. 2 The Relationship of K-Values to Areal Coverage of Showers in the Mid-South. Jack Hollis and Kenneth E. Bryan - August 1965

No. 3 Some Notes on Waterspouts around the Lower Keys. R. Larry Mayne - August 1965

No. 4 Tornadoes Associated with Cyclones of Tropical Origin - Practical Features. E. L. Hill, William Malkin and W. A. Schulz, Jr. - September 1965

No. 5 Radar Echoes Associated with Waterspout Activity. Dorus D. Alderman - October 1965

No. 6 Probability Forecasting. Woodrow W. Dickey - October 1965

No. 7 Short Period Forecasting. Jeter A. Pruett - November 1965

No. 8 Southwest Texas Soaring Weather. David H. Owens - November 1965

No. 9 A Survey of Research in Agricultural Meteorology. Donald A. Downey - November 1965

No. 10 A Quick Look at the Results of One Month's Precipitation Probability Forecasting. George T. Gregg - January 1966

No. 11 Severe Storm Warning Systems in the Southern Region. Staff Members of Operations Division, Southern Region - February 1966

No. 12 The Lubbock Snowstorm of February 20, 1961. Billie J. Cook - April 1966

No. 13 Summary of Probability of Precipitation Forecasts in the Southern Region for the Period January through March 1966. Woodrow W. Dickey - May 1966

No. 14 Air Pollution Meteorology and Transport of Pollutants. Jose A. Colon - June 1966

No. 15 On the Mechanisms for the Production of Rainfall in Puerto Rico Jose A. Colon - June 1966

No. 16 Teletype Techniques and Presentation Procedures for Public Weather Circuits. Jack Riley - June 1966

No. 17 Summary of the Pre-FP - Post-FP Forecast Verification Experiment. Woodrow W. Dickey - June 1966

No. 18 Fire Weather in the Southeast. Richard A. Mitchem - July 1966

No. 19 Severe Storm Warning Networks in Oklahoma. Gerald J. Carter and W. O. Garrison - July 1966

(continued) LIST OF SOUTHERN REGION TECHNICAL MEMORANDA

No. 20 Climatological Aids to Short Range Forecasting. Jerome H. Codington - August 1966

No. 21 A review of the Methods Developed for Forecasting Stratus in South Central Texas. Richard S. Schrag - August 1966

No. 22 Agricultural Forecasting at Tallahassee, Florida. J. S. Smith - August 1966

No. 23 The Use of Radar in Flash Flood Forecasting. Jack L. Teague - August 1966

No. 24 Short Range Forecasting Procedures at Savannah. David P. Barnes - August 1966

No. 25 On the Use of Digitized Radar Data for the Florida Peninsula. Neil L. Frank Paul L. Moore and George E. Fisher - Sept. 1966

No. 26 Relative Humidity in Georgia. Horace S. Carter - Sept. 1966

No. 27 Study on Duration of measurable Precipitation at Birmingham. Hugh B. Riley - September 1966

No. 28 The Weather Distribution with Upper Tropospheric Cold Lows in the Tropics. Neil L. Frank - September 1966

No. 29 On the Correlation of Radar Echoes over Florida with Various Meteorological Parameters. Neil L. Frank and Daniel L. Smith - October 1966

No. 30 A study of the Diurnal Summer Wind System at Galveston, Texas. David H. George - December 1966

No. 31 A simple Inexpensive Degree-Hour Counter. D. R. Davis and Jerrell E. Hughes - March 1967

No. 32 An Objective Technique for Forecasting the Possibility of an Afternoon Summer Shower at Savannah, Georgia. David P. Barnes, Jr. and Samuel C. Davis - March 1967

No. 33 An Empirical Method for Forecasting Radiation Temperatures in the Lower Rio Grande Valley of Texas. Leroy B. Hagood - March 1967

No. 34 Study on Duration of Measurable Precipitation at Lubbock, Texas. G. Alan Johnson and Thomas P. Clarke - April 1967

No. 35 Remoting Radar Scope Weather and Associated Data via the Slo-Scan Method. Davis Benton - May 1967

No. 36 Short Range Forecasting of Dryoff Time From Dew Block Dew Intensity. Dorus D. Alderman and Kenneth E. Bryan - October 1967

No. 37 The Relationship of K-Values to Probability of Showers in the Mid-South. Kenneth E. Bryan - October 1967

No. 38 Florida Hurricanes. Gordon E. Dunn and Staff NHC, Miami November 1967